HHS Public Access

Author manuscript

Nat Neurosci. Author manuscript; available in PMC 2023 May 16.

Published in final edited form as:

Nat Neurosci. 2022 September ; 25(9): 1191–1200. doi:10.1038/s41593-022-01146-x.

Experimenters' sex modulates mouse behaviors and neural responses to ketamine via corticotropin releasing factor

Polymnia Georgiou[1,2,3], **Panos Zanos**[2,4], **Ta-Chung M. Mou**[2], **Xiaoxian An**[2], **Danielle M. Gerhard**[5,15], **Dilyan I. Dryanovski**[2], **Liam E. Potter**[2,6], **Jaclyn N. Highland**[2,7], **Carleigh E. Jenne**[2], **Brent W. Stewart**[2,8], **Katherine J. Pultorak**[8], **Peixiong Yuan**[9], **Chris F. Powels**[2], **Jacqueline Lovett**[10], **Edna F. R. Pereira**[11], **Sarah M. Clark**[1,2], **Leonardo H. Tonelli**[1,2], **Ruin Moaddel**[10], **Carlos A. Zarate Jr**[9], **Ronald S. Duman**[5], **Scott M. Thompson**[2,12], **Todd D. Gould**[1,2,13,14]

[1]Veterans Affairs Maryland Health Care System, Baltimore, MD, USA.

[2]Department of Psychiatry, School of Medicine, University of Maryland, Baltimore, MD, USA.

[3]Department of Biology, University of Cyprus, Nicosia, Cyprus.

[4]Department of Psychology, University of Cyprus, Nicosia, Cyprus.

[5]Department of Psychiatry, Yale University, New Haven, CT, USA.

[6]Michigan Neuroscience Institute, University of Michigan, Ann Arbor, MI, USA.

[7]The Graduate Program in Toxicology, University of Maryland, Baltimore, MD, USA.

Correspondence and requests for materials should be addressed to Todd D. Gould. gouldlab@me.com.

Author contributions

P.G. and T.D.G. were responsible for the overall experimental design. T.M.M. and K.J.P. performed the RNAscope experiments. T.M.M. performed automated RNAscope analysis with supervision by L.H.T. and S.M.C. D.M.G. and R.S.D. performed the independent FST replication at Yale University. C.F.P. and X.A. perfused mice and processed the brains for expression and cannula implantation confirmation. D.I.D. performed the whole-cell electrophysiology experiment with supervision from E.F.R.P. L.E.P. and P.G. performed analysis for the fiber photometry experiments. C.E.J. and B.W.S. performed qEEG surgeries. B.W.S. and P.G. performed qEEG data analysis. C.E.J. performed the FST. P.Z., J.N.H., P.G., B.W.S. and S.M.C. performed the PK studies (injections, euthanasia and tissue collection) and experiments utilizing single experimenters. R.M. and J.L. conducted bioanalytical quantitation of ketamine and metabolites. P.Y. and C.A.Z. performed the western blot experiments. S.M.T. helped design and analyze the electrophysiological experiments. P.G. conducted the experiments and their analysis unless otherwise noted. P.G. and T.D.G. outlined and wrote the paper, which was reviewed by all authors.

Reporting summary. Further information on research design is available in the Nature Research Reporting Summary linked to this article.

Online content

Any methods, additional references, Nature Research reporting summaries, source data, extended data, supplementary information, acknowledgements, peer review information; details of author contributions and competing interests; and statements of data and code availability are available at https://doi.org/10.1038/s41593-022-01146-x.

Competing interests

C.A.Z. is a co-inventor on a patent for the use of ketamine in major depression and suicidal ideation. P.Z., J.N.H., R.M., C.A.Z. and T.D.G. are co-inventors in patents or patent applications related to the pharmacology and use of (*2R,6R*)-HNK in the treatment of depression, anxiety, anhedonia, suicidal ideation and post-traumatic stress disorders. R.M. and C.A.Z. have assigned their patent rights to the US government but will share a percentage of any royalties that may be received by the government. P.Z., J.N.H. and T.D.G. have assigned their patent rights to the University of Maryland Baltimore but will share a percentage of any royalties that may be received by the University of Maryland Baltimore. T.D.G. has received research funding from Allergan and Roche Pharmaceuticals and has served as a consultant for FSV7 LLC, during the preceding 3 yr. All other authors declare no competing interests.

Supplementary information The online version contains supplementary material available at https://doi.org/10.1038/s41593-022-01146-x.

[8]The Graduate Program in Neuroscience, University of Maryland, Baltimore, MD, USA.

[9]Experimental Therapeutics and Pathophysiology Branch, Intramural Research Program, National Institute of Mental Health, National Institutes of Health, Bethesda, MD, USA.

[10]Biomedical Research Center, National Institute on Aging, National Institutes of Health, Baltimore, MD, USA.

[11]Department of Epidemiology and Public Health, School of Medicine, University of Maryland, Baltimore, MD, USA.

[12]Department of Physiology, School of Medicine, University of Maryland, Baltimore, MD, USA.

[13]Department of Pharmacology, School of Medicine, University of Maryland, Baltimore, MD, USA.

[14]Department of Anatomy and Neurobiology, School of Medicine, University of Maryland, Baltimore, MD, USA.

[15]Present address: Department of Psychiatry, Weill Cornell Medicine, New York, NY, USA.

Abstract

We show that the sex of human experimenters affects mouse behaviors and responses following administration of the rapid-acting antidepressant ketamine and its bioactive metabolite (*2R,6R*)-hydroxynorketamine. Mice showed aversion to the scent of male experimenters, preference for the scent of female experimenters and increased stress susceptibility when handled by male experimenters. This human-male-scent-induced aversion and stress susceptibility was mediated by the activation of corticotropin-releasing factor (CRF) neurons in the entorhinal cortex that project to hippocampal area CA1. Exposure to the scent of male experimenters before ketamine administration activated CA1-projecting entorhinal cortex CRF neurons, and activation of this CRF pathway modulated in vivo and in vitro antidepressant-like effects of ketamine. A better understanding of the specific and quantitative contributions of the sex of human experimenters to study outcomes in rodents may improve replicability between studies and, as we have shown, reveal biological and pharmacological mechanisms.

The inability to replicate experimental results between, and sometimes within, laboratories may be due to unrecognized experimental variables that are not appropriately controlled[1]. The sex of the human experimenter is rarely considered as a biological variable that can affect experimental results and is often not accounted for by design, included as a factor in statistical analyses or reported in experimental methods[2-4]. However, there is evidence that the ability of rodents to differentiate the sex of human experimenters can have measurable effects on their behavioral and/or biological responses[2-4]. For instance, exposure of rodents to male, but not female, experimenters' scent has been shown to increase anxiety-related behaviors and stress-induced analgesia[2]. Here, we investigated the role of the experimenter's sex on stress-induced maladaptive behaviors and how scent from male versus female experimenters might affect rodent biobehavioral responses to pharmacological antidepressant treatments (see Supplementary Table 1 for details on experimental designs, statistical tests used and group sizes).

Results

Human experimenter scent modulates behavioral responses.

We first assessed whether CD1, BALB/c or C57BL/6J mice prefer to interact with a cotton swab rubbed across the skin (cubital fossa, inner wrist and mastoid) of human males compared with human females. The sex of volunteer human experimenters was recorded based on self-identification and we use the term 'sex' to refer to this reported classification. Mice of both sexes consistently exhibited preference to the female-scented swabs (Fig. 1a). This preference was likely smell driven, because it was not observed in mice rendered anosmic by intranasal treatment with zinc sulfate (Fig. 1b). Also, when given the choice between a swab dampened with water (control scent) versus human male or female skin-exposed swabs, mice showed aversion to male swabs, whereas they displayed preference for female swabs (Fig. 1c). Likewise, in a real-time place preference paradigm, mice showed avoidance to t-shirts that had been worn by male experimenters, whereas they showed preference for t-shirts that had been worn by female experimenters (Fig. 1d and Supplementary Video 1).

To directly compare the behavioral response of mice to male, female and control scent we used a Y-shaped maze. We attached one swab to one of the three arms of the maze and measured the time mice spent in each arm. In agreement with results in Fig. 1a-d, mice spent less time in the maze arm containing the male-experimenter-exposed swab compared with either the control arm or the arm containing the female-experimenter-exposed swab (Fig. 1e,f). No difference was observed in the time spent between the arms containing control versus female experimenter swabs (Fig. 1e,f).

To test the specific rewarding or aversive properties of male versus female experimenter scent, mice were assessed for conditioned place preference/aversion. Mice were exposed to different scents in two distinct compartments within a two-compartment chamber and were subsequently assessed for any conditioned preference. Male experimenters' scent induced place aversion (Fig. 1g,h), suggesting that male-experimenter scent has an aversive aspect; however, neither place preference nor aversion was observed following exposure to female experimenters' scent (Fig. 1g,h), suggesting that female scent may not be directly rewarding. We performed additional analyses of the scent-related experiments (Fig. 1a-h) using receiver operating characteristic (ROC) curves. An ROC curve is an analysis for binary classifiers, in our case male or female/control experimenters, to demonstrate whether the effects are more likely to be true or more likely to be false. We found that the ROC curve fit is robustly above the chance line, indicating that the effect of male experimenters is a true positive (Fig. 1i; see also effect size analyses provided in Supplementary Table 2).

To determine whether scents from male versus female experimenters affect behavioral responses to stress, we investigated the effect of exposure to male or female experimenters on behavior in a forced-swimming test (FST). In the FST, mice were placed into a water-containing, escape-proof cylinder and their resilience in adopting a helpless floating posture was timed[5]. Mice handled by male experimenters showed significantly longer immobility time compared with those handled by female experimenters (Extended Data Fig. 1a; pooled results from all FST experiments presented in this manuscript), suggestive of a greater

stress response induced by male experimenters. In the sucrose splash test, in which the time to initiate grooming is measured after mice are sprayed with high-concentration sucrose-containing water, we also observed a longer latency for mice to groom in the presence of swabs containing male-experimenter scent versus swabs containing female experimenter scent (Fig. 1j). These findings are indicative of mice presenting decreased self-care, a corollary manifestation of increased stress[6], when exposed to swabs from male experimenters.

Similarly, we observed a greater latency for mice to eat in the novelty-suppressed feeding test when the experiment was performed by male versus female experimenters (Fig. 1k), which is also indicative of greater anxiety in the presence of male experimenters[7]. Furthermore, increased escape deficits following exposure to inescapable footshock training were observed when CD1 (Fig. 1l,m) or CFW Swiss Webster (Extended Data Fig. 1b,c) mice were handled by male versus female experimenters, suggesting that handling of male and female mice by male experimenters increases helplessness-like behavior. Similarly, when male and female experimenters subjected male C57BL/6J mice to a chronic social defeat stress (CSDS) paradigm (consisting of daily exposure to a larger aggressive mouse for 10 d), mice handled by male experimenters showed lower sucrose preference (suggestive of anhedonia) than mice handled by female experimenters (Extended Data Fig. 1d). By contrast, there was no effect of experimenters' sex on behavior in the light–dark preference test, which tests for anxiety-like behavior (Extended Data Fig. 1e). These findings extend those by Sorge et al.[2], by demonstrating that the sex of the human experimenter affects not only anxiety and pain responses[2] but also depression-relevant behaviors in mice. The findings suggest that the sex of human experimenters may more broadly be considered a factor that can influence rodent behavior and experiments that measure behavioral outcomes.

Experimenters' sex affects pharmacological treatments.

The finding that human experimenters' sex influences mouse behaviors raises the question of whether it also affects the responses of mice to experimental manipulations, including pharmacological treatments. To address this question, we assessed the effects of experimenters' sex on mouse responses to (*R,S*)-ketamine (KET) administration. KET is an effective rapid-acting antidepressant at subanesthetic doses clinically and its antidepressant-like actions were also observed in preclinical rodent models[8-11]. Under our routine laboratory testing conditions[8,12-15], we found that, among five distinct pairs of experimenters, KET injected by male, but not female, experimenters decreased immobility time in male CD1 mice tested 1 h post-treatment (Fig. 2a). This effect of the experimenter's sex on responses to KET was also observed in male mice subjected to the FST 24 h postinjection (Extended Data Fig. 2a), in female CD1 mice (Extended Data Fig. 2b) and in mice exposed to a pre-swim session 23 h before drug injection and 24 h before re-exposure to the FST (Extended Data Fig. 2c). In addition, KET administered by a male, but not a female, experimenter reversed CSDS-induced sucrose preference deficits in male C57BL/6J mice (Fig. 2b; days 1–3). After sucrose preference returned to normal levels, re-exposure to a brief 1-min social defeat session resulted in a reinstated reduction in sucrose preference in both female and male experimenter-handled mice that had previously received vehicle (Fig. 2b; days 9–12). However, mice that previously received KET treatment by a male, but not a

female, experimenter demonstrated a protective phenotype against stress-reinstated sucrose preference deficits (Fig. 2b; days 9–12). When CD1 and CFW mice were administered KET by a male, but not a female, experimenter, their escape deficits induced by inescapable shock were also significantly decreased 24 h following treatment (Fig. 2c and Extended Data Fig. 2d).

We were aware that other laboratories have anecdotally made similar observations. Therefore, another randomized and blinded study for an effect of the sex of experimenters injecting KET was repeated at Yale University by eight male and eight female experimenters (Fig. 2d and Extended Data Fig. 2e). In line with our observations, administration of KET by male but not female experimenters in mice decreased immobility time in the FST (Fig. 2d and Extended Data Fig. 2e). We note that within each sex, there was variability in the response indicative of other factors beyond the sex of the experimenter. Considering the breadth of KET research conducted previously in rodents[10,16-19], we also consider it probable that the all-or-nothing response to KET we find dependent on experimenters' sex is likely mediated by specific environmental, rodent strain and other unique conditions within laboratories. However, the differential antidepressant responses were not due to female experimenters altering the pharmacokinetics of KET, affecting circulating levels of its norketamine and (*2R,6R; 2S,6S*)-hydroxynorketamine (HNK) metabolites (Fig. 2e), or causing a rightward shift in the dose–response relationship for KET to suppress depression-related phenotypes (Extended Data Fig. 2f).

The action of KET as an *N*-methyl-D-aspartate receptor (NMDAR) antagonist accounts for many of its side effects, including hyperexcitability[20]. To determine whether the effects of experimenters' sex on behavioral responses to KET are specific to the antidepressant-relevant effects of the drug, we also assessed hyperlocomotion following KET administration. We observed an identical increase in locomotor activity following administration of KET to mice by a male or female experimenter (Extended Data Fig. 3a,b). This finding suggests that sex of the experimenter-mediated differences in antidepressant-like responses are not directly related to NMDAR inhibition. Consistent with this conclusion, administration of the NMDAR antagonist MK-801 by both male and female experimenters decreased immobility time in the FST 1 h postinjection (Extended Data Fig. 3c).

(*2R,6R*)-HNK is a pharmacologically active KET metabolite that is currently being evaluated in clinical trials to assess its safety and effectiveness for patients suffering from depression. It shares the antidepressant-like actions of KET in preclinical studies[8,13-15,17-24], but has low potency for NMDAR inhibition[15]. Administration of (*2R,6R*)-HNK by male experimenters reduced immobility in the FST. Regardless of the test dose, (*2R,6R*)-HNK had no effect on immobility when administered by female experimenters (Fig. 2f and Extended Data Fig. 3d,e). By contrast, administration of the classical tricyclic antidepressant desipramine reduced immobility in the FST when administered by either a male or female experimenter (Extended Data Fig. 3f). We also demonstrated that KET injected within a biosafety cabinet by gowned, isolation sleeved and gloved experimenters—an experimental condition that eliminates experimenter scent—had no effect on immobility in the FST regardless of the sex of the experimenter (Extended Data Fig. 4a). Altogether,

these data support an interaction between exposure to male experimenters' scent and KET's antidepressant-like behavioral effects. In line with this, when a female experimenter administered KET or vehicle within a biosafety cabinet in which male-worn t-shirts were placed by the mice, we observed a decrease in immobility time in the FST in the KET treatment group compared with the vehicle group (Extended Data Fig. 4b).

KET's mechanism of action for its antidepressant properties is still debated. One of the most prominent hypotheses is that it enhances hippocampal glutamatergic neurotransmission through AMPA receptors (AMPARs). Studies have reported that in rodents, expression of the AMPAR GluA1 subunit in the hippocampus is increased 24 h after administration of KET, and AMPAR activity is required for KET's antidepressant-relevant behavioral effects[8-11]. In line with this, we found increased synaptic GluA1 AMPAR subunit levels in the ventral hippocampus of mice 24 h after administration of KET by male, but not female, experimenters (Fig. 2g and Supplementary Fig 1).

The ventral hippocampus is known to drive neuronal activity in the prefrontal cortex, a brain region thought to be critically involved in KET's antidepressant effects[25]. Since antidepressant-relevant doses of KET increase the power of cortical gamma oscillations[26], we used quantitative electroencephalography (qEEG) to determine whether experimenters' sex influences the effects of KET on prefrontal cortical electrical activity. Consisted with previous reports, KET increased qEEG power in the 30–120-Hz range (Fig. 2h-k); however, this effect of KET was greater when male experimenters administered the KET (Fig. 2h-k and Extended Data Fig. 5a-f).

CRF mediates the effect of experimenters' sex.

Acute exposure of mice to male experimenter scent has been reported to increase hypothalamic–pituitary–adrenal (HPA) axis activity, as evidenced by higher plasma corticosterone levels[2]. However, we found that inhibition of corticosterone synthesis by pretreatment with metyrapone, a reversible inhibitor of steroid 11β-hydroxylase, did not prevent the behavioral effect of KET administered by male experimenters in CD1 mice (Extended Data Fig. 6a). Since CRF is released following HPA axis activation and precedes the corticosterone response[27], we examined whether CRF could mediate the effects of experimenter scent on the antidepressant-like responses to KET.

Intracerebroventricular (ICV) administration of CRF before administration of KET within a biosafety cabinet by a female experimenter resulted in decreased immobility time in the FST 24 h later (Fig. 3a) and in fewer escape failures in a learned helplessness paradigm in KET- (Fig. 3b) and (*2R,6R*)-HNK-treated (Fig. 3c) mice. In line with these findings, peripheral administration of the brain-penetrant CRF receptor 1 (CRFR1) antagonist CP-154,526 blocked antidepressant-like effects of male experimenter-administered KET in the learned helplessness paradigm (Fig. 3d), FST (Fig. 3e) and in a sucrose preference test following CSDS (Fig. 3f). Furthermore, treatment with CP-154,526 decreased the aversion of mice to male experimenters' skin swabs (Fig. 3g,h) and abolished KET-induced increases in 30–120-Hz cortical oscillations (Fig. 3i-l and Extended Data Fig. 7a-f).

Based on these findings, we hypothesized that BALB/c mice, which display higher baseline immobility time in the FST compared with CD1 and C57BL/6J mice and have greater sensitivity to the behavioral effects of CRF[28,29], would display antidepressant-like responses to female-administered KET. Indeed, in BALB/c mice KET injected by either male or female experimenters decreased immobility time in the FST (Extended Data Fig. 6b), and pretreatment with CP-154,526 by a female experimenter blocked KET's effect on immobility (Fig. 3m). Overall, these findings suggest that male scent engages the CRF system, which results in a corticosterone synthesis-independent enhancement of stress responses, which in turn enables KET's antidepressant-like effects.

It was previously demonstrated that bath application of KET and (*2R,6R*)-HNK increases AMPAR-mediated potentiation in the Schaffer collateral (SC) pathway of the hippocampus[8,10,16,30,31], which is hypothesized to be relevant to its antidepressant response. We found that the AMPAR subunit GluA1 was increased in the hippocampus only when KET was administered by male experimenters (Fig. 2g). This suggested that the hippocampus might be involved in the effect of experimenters' sex. Thus, to identify a potential mechanism underlying the interaction between CRF and antidepressant-related KET responses, we recorded hippocampal CA1 field excitatory postsynaptic potentials (fEPSPs) following stimulation of either the SC pathway or the projections from the entorhinal cortex (EC) in hippocampal slices. Similar to our previous findings[8,30,31], we found that the KET metabolite (*2R,6R*)-HNK increased AMPAR-mediated fEPSPs following stimulation of the SC–CA1 pathway, but not the EC–CA1 projections (Fig. 4a,b and Extended Data Fig. 8a,b). Since CRF has been reported to prime long-term potentiation in the hippocampus[32,33], we hypothesized that CRF may enhance the fEPSP potentiation induced by (*2R,6R*)-HNK. CRF had no significant effect on (*2R,6R*)-HNK-induced potentiation of SC–CA1 fEPSPs (Extended Data Figs. 8a,b and 9a-e). However, combined with (*2R,6R*)-HNK it induced a potentiation of (*2R,6R*)-HNK-nonresponsive EC–CA1 synapses (Fig. 4c,d). This EC–CA1 fEPSP potentiation (Fig. 4e,f) by the combination of CRF and (*2R,6R*)-HNK was blocked by previous bath application of the CRFR1 antagonist CP-154,526.

Since our fEPSPs data suggest that CRF is necessary for the (*2R,6R*)-HNK potentiation of EC–CA1 synapses, we hypothesized that there is a CRF-expressing neuronal projection from the EC to CA1 which might be important for KET's antidepressant effects. First, we performed tracing studies to investigate whether EC to CA1 projection expresses CRF. In CRF-cre mice a cre-dependent retrograde fluorescent virus (AAV pCAG-FLEX-tdTomato-WPRE) was injected into the ventral CA1 and a CRF-expressing neuronal projection was identified from the EC to CA1 (Fig. 4g). We confirmed this finding in wild-type mice that received retrograde conjugated cholera toxin (CTb) injection into the ventral CA1 and RNAscope in situ hybridization of CRF transcripts was performed in the EC to test for colocalization of the CTb and CRF, revealing 10–18% colocalization, with no notable difference between medial and lateral EC or anterior and posterior EC (Extended Data Fig. 9a-h). Using whole-cell patch-clamp electrophysiology, we recorded postsynaptic currents (PSCs) from CA1 interneurons in the stratum lacunosum-moleculare (where CRF EC projections terminate) in response to photostimulation of the presynaptic EC–CRF projection terminals in coronal brain slices obtained from CRF-cre mice that received

an injection of a Cre-sensitive channelrhodopsin-2 (ChR2)-expressing vector into the EC (Fig. 4h,i). These PSCs were glutamatergic in nature because they were (1) recorded from neurons that were voltage clamped at −60 mV and dialyzed with a methanesulfonate-based internal solution that shifted the reversal potential for GABA to approximately −50 mV, and (2) blocked by superfusion of the slices with artificial cerebrospinal fluid (ACSF) containing the NMDA and AMPAR antagonists 2-amino-5-phosphonopentanoic acid (DL-AP5) and 6,7-dinitroquinoxaline-2,3-dione (DNQX), respectively.

To test the hypothesis that activation of CRF-expressing neurons projecting from EC–CA1 mediates the antidepressant effects of KET, mice received injections of YFP- or ChR2-expressing virus into the EC. After recovery, the mice received optogenetic stimulation of CRF terminals in the CA1 of the EC–CA1 pathway for 5 min followed by an injection of KET or vehicle. This experiment was performed by female experimenters within a biosafety cabinet to eliminate human odors and was designed to mimic the brief exposure to male experimenters before the administration of KET which results in antidepressant effects. Optogenetic activation of the EC–CA1 CRF projection combined with KET administration resulted in decreased immobility time in the FST (Fig. 4j), demonstrating that activation of this projection is sufficient to induce similar effects to exposure to male scent, thereby priming mice to respond to the antidepressant-like effects of KET.

Previous studies reported that the EC is an important region for olfactory cue processing and discrimination[34,35]. Thus, we hypothesized that male scent activates CRF neurons projecting from the EC to the CA1, thereby priming the EC–CA1 synapses to the potentiating effects of (*2R,6R*)-HNK and KET. Accordingly, we observed an increase in the number of CRF transcripts and CRF/Fos colabeled cells, but no difference in total Fos transcripts, in the EC following exposure to swabs exposed to male skin (Fig. 5a-d). This finding supports the notion that human male scent induces activation of CRF neurons in the mouse EC. To investigate the involvement of this projection in the observed mouse aversion to the male experimenters' scent, we tested whether activation of the CRF EC–CA1 projection mimics the aversion induced by male scent in a real-time place preference assay. Photostimuli were applied to the CA1 region of ChR2- and YFP-expressing mice when they were within the assigned compartment of a two-compartment arena (Fig. 5e). Photostimulation of the CRF EC–CA1 projection in ChR2-expressing mice induced real-time aversion (Fig. 5f), similar to the aversion observed in response to the scent of male experimenters (Fig. 1e,f). Overall, these data demonstrate that exposure to male scent results in the activation of the EC CRF neurons and that photoactivation of the CRF EC–CA1 projection exerts aversive effects similar to the male-induced aversion.

We next addressed if inhibition of EC–CA1 transmission could reverse the aversion to the swabs with human male scent (Fig. 5g); if so, this would indicate that EC–CA1 transmission is necessary for the male-experimenter-induced aversion. Indeed, aversion to male-experimenter scent was reversed by systemic administration of clozapine N-oxide (CNO) before exposure to the scent in CRF-ires-cre mice in which cre-sensitive inhibitory Designer Receptors Exclusively Activated by Designer Drugs (DREADDs; DIO-hM4Gi-mCherry) were injected into the EC (Fig. 5g,h). This indicates that activity of CRF^{+} neurons in the EC mediates the adverse response of mice to male experimenters' scent (Fig. 5g,h).

Next, we assessed whether the activity of EC–CA1 neurons is associated with male scent exposure by recording calcium transients from the CRF^+ neurons in the EC using in vivo fiber photometry. CRF-ires-cre mice received an injection of a retrograde cre-sensitive jGCaMP7s bilaterally into the CA1. Following sufficient time for expression, mice were placed in a Y-maze apparatus, each arm containing a swab containing human male scent, a swab containing human female scent or a control swab, while calcium signals were simultaneously recorded from the soma of CRF^+ EC-CA1 projecting neurons (Fig. 5i). Activity of these neurons increased when mice were in the arm containing the male-scent swab compared with when they were in arms containing the female-scent swab or the no-scent (control) swab (Fig. 5j). Together, these data substantiate the conclusion that the CRF EC–CA1 pathway in mice is responsive to human male scent.

Discussion

Our data show that exposure to male versus female experimenters' scents induces differential behavioral responses and alters responses to antidepressant-relevant doses of KET in mice. Our results are in line with earlier findings of Sorge et al. which demonstrated that exposure to the scent of male experimenters resulted in higher corticosterone levels, stress-induced analgesia and increased anxiety-like behaviors in mice[2]. Furthermore, our findings show that aversion of mice to human male scents is due to activation of CRF-expressing neurons that project from the EC to CA1 and that this pathway underlies the differential behavioral responses of mice to male versus female experimenters.

Our data also reveal that sex of the experimenters affects not only baseline behaviors but also responses of mice to pharmacological treatments. This discovery enabled an in-depth dissection of a mechanism involved in the antidepressant-like effect of KET. In short, exposure of mice to male scent before KET administration activates CRF-expressing cells in the EC that project to CA1, priming this pathway to KET's antidepressant-relevant effects both in vivo and in vitro (Supplementary Fig. 2). Of note, our intention was not to characterize the EC as a brain region for processing human male scent as its role in scent mechanisms has previously been delineated[34-38], but rather to understand the interaction between human male scent and the antidepressant responses to KET. We initially hypothesized that stressing mice through traditional means—such as chronic social defeat, inescapable shock or pre-swim stress—before KET administration by a female experimenter would be sufficient for KET to induce an antidepressant-like effect. However, this was not the case under our laboratory conditions (Fig. 2b,c and Extended Data Fig. 2c), suggesting that it is the specific activation of the CRF projection from EC to CA1 that interacts with KET to induce its antidepressant effects. Thus, we postulate, as supported by our data (e.g. Fig. 4j), that KET administered by a female experimenter will have antidepressant-like effects provided the injection is preceded by a stressor or other manipulation that activates the CRF EC–CA1 projection.

Our findings suggest that acute KET/(*2R,6R*)-HNK combined with CRF receptor agonists may be a novel treatment approach for mood disorders. Specifically, we show that activation of the CRF EC–CA1 pathway is an important determinant of the antidepressant effects of KET. We hypothesize that the synergistic effect of KET and activation of this pathway

involves a cyclic AMP-dependent mechanism, relying on the G_s-coupled CRF1 receptor facilitating (*2R,6R*)-HNK-induced increase in the probability of glutamate release[30] through G-protein-coupled receptors. Indeed we previously demonstrated that inhibition of the G_i-coupled mGluR2 is necessary for the antidepressent effects of KET and (*2R,6R*)-HNK (ref. [13]).

Our study highlights the relevance of the sex of the human experimenter with regard to the replicability and the interpretation of results within and between laboratories. In our case, male experimenter-triggered stress responses resulted in an expected outcome (antidepressant-like effects of KET); it is possible that in other studies female experimenters may be more likely to obtain the historically expected results. For example, it was previously reported that exposure to male experimenters resulted in stress-induced analgesia that, in turn, dampened the anticipated pain response of mice and rats[2]. Many other factors may affect behavioral results or contribute to potential effects of experimenters' sex on experimental outcomes[1,39]. Such factors include, but are not limited to, ventilated versus open-air cages, use of rodents generated from in-house breeding versus rodents shipped from commercial suppliers, overall stress exposure within the facility, the phase of the circadian cycle in which animals are tested, unique handling procedures, the strain and substrain of the mice used, stress level of experimenters, diet of experimenters (meat-eaters versus plant-based diets) and the hormonal status of experimenters and/or animals. Controlling these factors and understanding how, specifically and quantitatively, they affect different experimental outcomes may lead not only to reduced heterogeneity between studies, but, equally important, to the discovery of novel biological mechanisms to advance scientific knowledge and drug discovery.

Methods

Experimental design.

All experiments were performed in a randomized manner (simple and stratified methods) by drug treatments and experimenters' biological sex. Experiments were determined not to require internal review board approval on the condition that no data other than biological sex were associated with or collected from human experimenters. Required samples sizes were estimated based upon our past experience performing similar experiments[5,8,13,14,30,31]. Mice were used for single experiments, that is, none of the mice were re-used for other experiments. Analyses of all experiments that included group comparisons were performed by experimenters blind to group assignments. Experimenters performing the injections and the behavioral procedures were also blind to the experimental groups. Experimenters did not have showers on the morning of the experiments and were not wearing perfumes or any other scented cosmetics/personal hygiene products on the day of the experiments. All handling of mice and injections for behavioral experiments were performed in the animal vivarium. Mice were only handled by the assigned experimenters during the experiments. In our institution, the animal care staff always open the cages within biosafety cabinets as specified by their standard operating procedures. Also, their personal protective equipment (PPE) specifications include oversleeves as well as long-sleeved gloves when working within the biosafety cabinet. Importantly, we do not allow the mice to be touched by anyone

for 2 d before the experiment. Thus, the mice should not encounter the smell of the animal caretaker performing the cage changes or food/water refilling. In our facility, cages are changed once every 2 weeks. Experiments were arranged at least 3 d after the cage change. Moreover, as a precaution 2 d before the experiment, special cage cards were placed on the cages specifying not to change cages.

All mice were weighed by the assigned experimenter a day before behavioral testing. No entrance by others was permitted during this time, only by the experimenters during their assigned injection/experiment time. Injections by the male and female experimenters alternated every 30 min to ensure that the room was free from the previous human experimenter's scent. Experiments in Figs. 1, 2d,f,g,h-k, 3g,h and 5a-d consisted of multiple male and female experimenters; each experimenter performed experiments with multiple mice (see Supplementary Table 1 for exact numbers of experimenters and mice) and the average outcome score of the mice from each experimenter was calculated (that is, biological replicates) for statistical analyses. Experiments requiring a biosafety cabinet were performed in a class II type A2 cabinet equipped with a high efficiency particulate air (HEPA) filter. The supply filter was a HEPEX Seal with 99.99% effectiveness on 0.3-μm-sized particles. The exhaust filter was a Neoprene, spring-loaded filter with 99.99% effectiveness on 0.3-μm-sized particles. The personal protective equipment of experimenters injecting within a biosafety cabinet included a single-use lab coat on top of the regular clean lab coat and high-sleeve gloves that were worn above the lab coat's sleeves.

Animals.

Mice (8 weeks old at arrival) were housed 4–5 per cage under a 12-h light–dark cycle (lights on at 7:00). Food and water were available ad libitum. Mice were housed in a temperature- (22.5 ± 0.5 °C) and humidity- (~44%) controlled environment. Mice were always housed in the same relative space on the racks, and the location of each group was always randomized within that space. Mice were acclimated to the animal vivarium for at least 7 d, and experiments were performed in 9–12-week-old animals. We have performed experiments with both male and female mice to assess if the phenomenon we describe exists in both sexes. When we determined that there is no sex difference, then we pursued with using male mice. For the circuit manipulation studies with the CRF-ires-cre mice, we used both male and female mice in all studies. CD1, CFW and BALB/c mice were obtained from Charles River Laboratories, while C57BL/6J were obtained from a colony maintained at the University of Maryland Baltimore Veterinary Resources. Breeding pairs for the CRF-ires-cre colony were kindly donated by Dr. Dennis Sparta (University of Maryland Baltimore) and initially purchased from the Jackson Laboratory. Wild-type, heterozygous and homozygous CRF-ires-cre were produced in-house by breeding heterozygous males and females or by breeding male and female homozygous CRF-ires-cre mice with wild-type mice. Tail samples from CRF-ires-cre were obtained before weaning and genotyped by TransnetYX. All experimental procedures were approved by the University of Maryland, Baltimore or Yale University Animal Care and Use Committees and were conducted in full accordance with the National Institutes of Health Guide for the Care and Use of Laboratory Animals.

Drugs.

(*R,S*)-KET, desipramine, (+)-MK-801, CRF (h/r) (all purchased from Sigma-Aldrich) and (*2R,6R*)-HNK (provided by the National Center for Advancing Translational Science) were dissolved in sterile saline (SAL) (0.9% NaCl; Quality Biological). CP-154,526 (Abcam) was dissolved in 20% ethanol in SAL and briefly heated at 60 °C. Metyrapone (Cayman Chemical) was dissolved in 5% Tween-20 in SAL. All drugs were administered intraperitoneally (i.p.) except for CRF, which was administered intracerebroventricularly at a volume of 1 μg in 4 μl. Injection volume for all drugs was 7.5 ml kg^{-1} except CP-154,526, which was 1.5 ml kg^{-1}.

Unless otherwise noted in the figure legends, drugs were administered at the following doses: (*R,S*)-KET (10 mg kg^{-1}), desipramine (20 mg kg^{-1}), (+)-MK-801 (0.03 mg kg^{-1}), CRF (h/r) (1 μg in 4 μl), (*2R,6R*)-HNK (10 mg kg^{-1}), CP-154,526 (30 mg kg^{-1}) and metyrapone (30, 50 and 70 mg kg^{-1}).

Surgical procedures.—In all surgical procedures, mice were anesthetized with isoflurane (induction: 3.5%; maintenance: 2–2.5%; VetOne). Analgesia was provided to the mice in the form of carprofen (5 mg kg^{-1}; subcutaneously (s.c.); Norbrook Laboratories) before the start of surgery and after the surgery once per day for 3 consecutive days.

Male/female experimenter scent sniffing preference test.

Clean cotton-tipped applicators (VWR) were firstly dipped in distilled water and then skin swabs were taken from cubital fossa, inner wrist and mastoid, and immediately placed in separate air-tight bags by each experimenter while using gloves. Applicators were used within 2 h of collection. Two applicators were used per experimenter. Each scent-containing applicator (swab) was used for two mice. This experiment was performed in clean cages placed on air-ventilated racks to avoid exposure of mice to other scents. First, mice were individually placed into clean cages for 10 min. Then, mice were habituated to a clean cotton-tipped applicator for 30 min. The cotton-tipped applicators were attached at their base to the top of the cage wall, with the tip oriented towards the center of the cage floor. Following habituation, the swabs with male or female experimenter scents were simultaneously introduced into the cage for 3 min. The time mice spent sniffing each swab was measured by an experimenter blind to the experimental groups. The cages were only opened within a biosafety cabinet when necessary for the experiment. Time sniffing each swab was scored live from an experimenter blind to the experimental groups.

Induction of anosmia.

Zinc sulphate ($ZnSO_4$) was used for the induction of anosmia, as previously described[40]. Mice were lightly anesthetized using isoflurane within a biosafety cabinet, and 10 μl of 5% $ZnSO_4$ or SAL was administered intranasally by placing the liquid on the base of the mouse's nostril. Intranasal administration occurred 1 h apart between each nostril. Behavioral testing occurred on the following day. Anosmia was confirmed by a food-finding task immediately after the male/female experimenter scent sniffing test. The food provided was chocolate-flavored sucrose pellets (Bioserv) and placed in the front corner of each cage. All of the $ZnSO_4$-treated mice were identified as anosmic (mean latency ± s.e.m.: SAL

= 18.44 ± 14.69 s; $ZnSO_4$, all mice reached the maximum testing time of 300 s without finding/eating the food provided).

Human experimenter versus control scent sniffing preference test.

This experiment was performed the same way as the male/female experimenter scent sniffing preference test. For the chemogenetic manipulation, CRF-ires-cre mice received an injection of 300 nl of AAV5-hSyn-DIO-hM4D(Gi)-mCherry or AAV5-hSyn-DIO-mCherry (Addgene) into the EC (Anterior-Posterior (AP): −2.8, Medial-Lateral (ML): ±4.25, Dorsal-Ventral (DV): −5.17 from the top of the skull). Four weeks following the injection into the EC, mice received vehicle (7.5 ml kg^{-1}; i.p.; 5% dimethylsulfoxide) 40 min before scent introduction. One week later, mice were treated with CNO (3 mg kg^{-1}; i.p.) 40 min before their exposure to scented swabs. CNO was dissolved in 5% dimethylsulfoxide and injections were performed within a biosafety cabinet. Sessions were recorded with a video camera and analyzed by an experimenter blind to the experimental groups.

Y-maze scent preference test.

The Y-maze apparatus (Stoelting) consists of three identical arms (5 × 35 cm) joined in the middle, forming a ‘Y’ shape. Mice were placed in the center of the equipment and allowed to explore the apparatus for 8 min. Following habituation, male experimenter-scented, female experimenter-scented and water swabs were attached at the end of each arm. Mice were re-introduced to the arena, now including the swabs, for 8 min. Locations of the scent swabs were counterbalanced. All the experimental trials were recorded with an overhead video camera and analyzed with TopScan (CleverSys) tracking software. The time spent in the area close to the swab, which equivalates 75% of the arm, was calculated.

Scent-induced real-time place preference.

The real-time place preference apparatus consists of a three-chambered rectangular box (two equal-sized end-chambers and a middle chamber; 40-cm length × 30-cm width × 35-cm height; Stoelting). A clear perforated plexiglass divider was placed in each end-chamber, separating them into two compartments. The t-shirts were beige color and folded the same way to occupy the same area between trials. They were placed in the compartment (10 × 15 × 36 cm) towards the end of the chamber away from the middle chamber so that the mice could not have direct physical interaction with the t-shirts. For this experiment we used t-shirts worn for 24 h. The t-shirts were never worn by anyone else before this experiment and they were washed with nonscented, hypoallergenic detergent. Experimenters placed the t-shirts in an air-tight bag in the morning of the experiment. During the real-time place preference test, the mouse was initially placed in the apparatus without the t-shirts and allowed to freely explore for 2.5 min. Following that, the t-shirts were introduced, and the mouse was allowed to continue exploration for another 2.5 min. The control and male- or female-worn t-shirts were counterbalanced with respect to chamber side during the experiment. A male experimenter performed the experiment with the male-worn t-shirts and a female experimenter performed the experiment with the female-worn t-shirts. The experimenters immediately left the testing room upon placement of the mice into the behavioral chamber during both habituation and testing. Each t-shirt was used for two mice and the average scores of those two mice were calculated for the final results per each

individual. The real-time place preference experiment was performed under low-lighting conditions (30 lux) and sessions were recorded using overhead cameras. An experienced experimenter blind to the experimental groups scored the amount of time mice sniffed the experimenter-worn t-shirt versus the control t-shirt.

Optogenetics-induced real-time place preference.

A three-chambered box (40-cm length × 30-cm width × 35-cm height; Stoelting) with smooth gray floor was used to measure mice's preference of the light-paired compartment to the non-light-paired compartment. One compartment had white vertical stripes 4 cm apart on each wall, while the other had white horizontal stripes 4 cm apart. Allocation of the light-paired compartment was counterbalanced to avoid any side preferences. Heterozygous CRF-ires-cre mice received 300-nl injections of AAV5. EF1a-DIO-eYFP-WPRE-hGH (Penn Vector Core) or AAV5.EF1a-DIO-hChR2(H134R)-eYFP-WPRE-hGH (Addgene), respectively, into the EC (AP: −2.8, ML: ±4.25, DV: −5.17 from the top of the skull) at a rate of 20 nl min^{-1} using a 1-μl Hamilton syringe (Knurled Hub Needle, 25 G), followed by implantation of the optic cannulas (Neurophotometrics) in the CA1 (AP: −2.3; ML: ± 3.25; DV: −4.5 from top of the skull) 3 weeks after virus infusion. At 10–15 d after implantations, ChR2- and YFP-injected mice were connected to optogenetic fiber cables (Doric Lenses), placed in the middle compartment and tracked by an overhead camera. During the 30-min testing period, mice that crossed into the allocated light-paired compartment received a 20-Hz continuous stimulation (470 nm, 200 μm, 0, 37 numerical aperture (NA), ~2–3 mW). Mouse crossings into each compartment were detected by a Bonsai script, which communicated to the light-emitting diode through a PulserPlus box (Prizmatix) for light delivery.

Conditioned place preference/aversion.

The same three-chambered apparatus as the one described for the real-time place preference experiment (40-cm length × 30-cm width × 35-cm height; Stoelting) was also used for the conditioned place preference/aversion paradigms. Removable doors were inserted to separate the apparatus into two equal-sized compartments. One compartment consisted of walls with white vertical stripes 4 cm apart and a smooth black floor and the other compartment consisted of black walls and a perforated floor. The protocol consisted of a pre-conditioning phase, three conditioning phases and a post-conditioning test. The lighting used for all phases of the experiments was 30 lux. During the pre-conditioning day, mice were placed in the middle chamber and allowed to freely explore the apparatus for 10 min. The conditioning phase consisted of 3 d with two conditioning sessions per day. During these sessions, mice were confined to a single compartment and exposed to human experimenter or control scent. Two cotton-tipped applicators with experimenter scents were secured with clear tape onto the walls of one of the compartments, 15 cm above the floor, during the morning sessions; control cotton applicators wetted with only distilled water were placed in the opposite compartment in a similar fashion during the afternoon sessions. Conditioning sessions lasted 10 min, and the top of the apparatus was covered using black Plexiglass to keep the smell of the swabs in the chamber as much as possible. Female scent was paired with the least-preferred compartment, which was defined during the pre-conditioning test, to assess for place preference, whereas male scent was paired

with the most-preferred compartment to assess for place aversion. Mice were serially exposed to scents from multiple experimenters of the same sex during each conditioning session. Collection of the cotton-tipped applicators containing human experimenter scent was performed as described earlier. During the post-conditioning test, mice were placed in the center chamber and allowed to freely explore the whole apparatus for 10 min. Time spent in each compartment was analyzed using TopScan video tracking software (CleverSys) during both the pre- and post-conditioning sessions for the last 5 min, as previously described[8].

Sucrose splash test.

Mice were placed in clean cages without bedding. Following 10 min of habituation in the cage, two cotton-tipped applicators from either a male or female experimenter were attached on the inside of the cage top using clear tape. The mice were sprayed with a 10% sucrose solution on their dorsal coat surface and latency to groom was scored by an experimenter blind to the treatment groups. This experiment was performed in a biosafety cabinet.

Novelty-suppressed feeding test.

Mice were singly housed and food deprived overnight in freshly made home cages that were prepared within a biosafety cabinet by a female or male experimenter. Water was available ad libidum. During the test day, one regular chow diet pellet was placed on an inverted petri dish platform in the center of an open-field arena (40 × 40 cm). Then, male or female experimenters placed their assigned mice in the arenas and left the room. There was a 30-min gap period between sessions to allow for the smell of the experimenters to be eliminated from the room. Sessions lasted 15 min, and behavior of mice was recorded by overhead video cameras for analysis. The latency for mice to take a bite of food was scored by a trained experimenter blind to the experimental groups.

Light/dark box.

Male or female experimenters placed mice in the illuminated compartment of the light/dark box (35 × 35 cm), facing the wall opposite to the dark compartment. Similar to previous experiments, trials from male and female experimenters were run interchangeably and there was a 30-min gap period between sessions to allow for the smell of the experimenters to be eliminated from the room. Mice were allowed to explore the whole apparatus for 10 min. The sessions were recorded using overhead video cameras and the time spent in the illuminated and the dark compartments was scored using TopScan v.2.0 (CleverSys). Each experimenter was assigned a cage of two male CD1 mice.

Footshock-induced escape deficits and reversal of escape deficits.

Induction.—The behavioral testing consisted of two phases: the inescapable shock training and screening for helplessness. Eight male and female experimenters were each assigned with two cages of five CD1 mice (five male and five female mice). For the inescapable shock training (day 1), the animals were placed in one side of two-chambered shuttle boxes (Coulbourn Instruments), with the door between the chambers closed. Following a 5-min adaptation period, 120 inescapable footshocks (0.45 mA, 15-s duration, randomized

average inter-shock interval of 45 s) were delivered. During the screening session (day 2), mice were placed in one of the two chambers for a 5-min adaptation period. After the adaptation period, a 0.45-mA shock was delivered with the door between the two chambers opening simultaneously. If the animal crossed over to the adjacent chamber, the shock was terminated, whereas if the animal did not cross over, the shock was terminated after 3 s. A total of 30 screening trials of escapable shocks were presented with an average of 30-s delay between each trial. Mice were considered helpless if they had more than or equal to five escape failures during the last ten screening shocks and more than or equal to twenty total escape failures.

Reversal.—For the escape deficits reversal experiments, we used the same paradigm as described by Zanos et al.[8]. Briefly, the protocol consisted of four phases: inescapable shock training, screening, treatment and the test. The training (day 1) and screening (day 2) sessions were performed as described above in the induction of escape deficits. Helpless mice that developed escape deficits, defined as having more than or equal to five escape failures during the last ten screening shocks and more than or equal to twenty total escape failures, were given an injection of either SAL or KET on day 3. CP-154,526 was administered 30 min before SAL/KET and CRF was administered a few seconds before SAL/KET. During the testing phase (day 4), the animals were placed in shuttle boxes and, after a 5-min adaptation period, a 0.45-mA shock was delivered concomitantly with door opening for the first five trials, followed by a 2-s delay for the next 40 trials. Similar to the screening session, the animal crossing over to the adjacent chamber terminated the shock; the shock was terminated after 24 s if the animal did not cross. Each mouse received a total of 45 trials of escapable shock with an average of 30-s inter-trial intervals. The number of escape failures was automatically recorded (Graphic State v.3.1).

All the phases of the footshock-induced escape deficits protocol as well as the treatments were performed by the same experimenter. Sessions by both male and female experimenters were run interchangeably with a 30-min time gap between experimenters to ensure that the room and equipment were free of human experimenter scent. Boxes were also cleaned in between sessions.

FST.

Mice were tested in the FST 1 h or 24 h postinjection. Pretreatments with metyrapone and CP-154,526 occurred 30 min before KET/SAL treatments in a biosafety cabinet. CRF was administered (ICV) at the same time as KET in the biosafety cabinet; ICV administration was performed as previously described[14]. Due to the use of a very brief isoflurane anesthesia, CRF-treated mice were tested only in the FST 24 h after drug administration. For the optogenetic stimulation, heterozygous CRF-ires-cre mice received 300-nl injections of AAV5.EF1a-DIO-eYFP-WPRE-hGH (Penn Vector Core, Addgene) or AAV5.EF1a-DIO-hChR2(H134R)-eYFP-WPRE-hGH (Penn Vector Core, Addgene), respectively, into the EC (AP: −2.8, ML: ± 4.25, DV: −5.17 from the top of the skull) at a rate of 20 nl min^{-1} using a 1-μl Hamilton Syringe (Knurled Hub Needle, 25 G), followed by implantation of the optic cannulas (Neurophotometrics) in the CA1 (AP: −2.3; ML: ±3.25; DV: −4.5 from top of the skull) 3 weeks after virus infusion. At 10–15 d following implantations, mice injected

with ChR2- and YFP-expressing vectors were connected to optogenetic fiber cables (200 μm, 0.37 NA; Doric Lenses). YFP- and ChR2-expressing mice received a 20-Hz stimulation of 470-nm light, ~2–3 mW, for 5 min before the injection with KET. Mice were tested in the FST 24 h postinjection. The FST was performed as previously described[8]. Briefly, mice were subjected to a 6-min FST session in clear Plexiglas cylinders filled to 15 cm with water (23 ± 1 °C) under normal lighting conditions (800 lux). The FST was recorded using a digital video camera. The FST was always performed by a female experimenter who did not perform injections in the same experiment. Immobility was defined as passive floating with no additional movements other than those necessary to stay afloat. Immobility time was scored for the last 4 min by a trained observer blind to the experimental groups.

In the 2-d FST experiment, mice were exposed to a 15-min pre-swim session on day 1. On day 2, mice were exposed to a 6-min swim session as described above. KET was administered 1 h before the testing session on day 2 and 23 h after the pre-swim session on day 1. Immobility time was scored for the last 4 min of the 6-min session on day 2 by a trained observer blind to the experimental groups.

In the FST experiment in which t-shirts were used, male experimenters were asked to wear the t-shirts for a 24-h period, after which t-shirts were placed in an air-tight bag until use. Control t-shirts were not worn by anyone. The t-shirts were placed within a biosafety cabinet and mice were scruffed for injections on the male-worn t-shirts by a female experimenter (so that mice could only smell the t-shirt and not the person injecting). At 1 h postinjection, mice were tested in the FST.

CSDS.

Male C57BL/6J mice underwent a 10-d CSDS paradigm, as previously described[8,13] with minor modifications. Briefly, experimental mice were introduced to the home cage of a resident aggressive, retired CD1 breeder for 10 min. Following this physical attack phase, mice were transferred and housed in the opposite side of the resident's cage separated by a perforated Plexiglas divider to maintain sensory contact for the remainder of the day. This process was repeated for 10 d, each day with a novel aggressive CD1 mouse. After the last defeat session on day 10, the C57BL/6J mice were singly housed in clean cages and returned to the animal vivarium. From day 10 to day 12, mice were tested for the development of anhedonia by assessing their preference for sucrose. Two pre-weighed bottles, containing either drinking water or 1% (w/v) sucrose solution, were introduced into the experimental C57BL/6J mouse cage. Water and sucrose consumption were measured by weight every day. Moreover, location of the bottles was switched every day following weight measurements to avoid development of place preference. Mice that had sucrose preference lower than 60% were given a single injection of either SAL (7.5 ml kg^{-1}) or KET (20 mg kg^{-1}) on day 12. Sucrose and water consumption were measured for 9 additional days, at the end of which time all mice recovered their preference; the sucrose bottle was then removed. On day 21, experimental C57BL/6J mice were placed in the home cage of a novel aggressive CD1 for 1 min to assess for reinstatement of sucrose preference deficits and possible prophylactic actions of previous KET administration. Sucrose consumption was measured daily for another 4 d.

The CSDS paradigm was run in parallel by a male and a female experimenter in two separate behavioral rooms, adjacent to each other and under the same lighting, temperature and humidity. Following the termination of the social defeat and the return of the mice to the animal vivarium for sucrose preference testing, the initial male and female experimenters were the only ones to open the cages and measure the sucrose and water consumption. Sucrose preference measurements were performed 30 min apart between each experimenter. The social defeat reinstatement phase was performed in two separate rooms by the same initial experimenters.

To test the role of CRFR1 in male-injected KET-mediated reversal of CSDS-induced sucrose preference deficits, only mice with baseline preference higher than 80% were used. The CSDS procedure was performed as described above and the mice were exposed only to the male experimenter running the experiment. CP-154,526 and vehicle (20% ethanol) were administered 30 min before KET/SAL administration.

Open-field test.

Mice were placed into individual open-field arenas (50 × 50 × 38 cm; San Diego Instruments) for a 30-min habituation period, administered a SAL injection by a male or female experimenter and assessed for locomotor activity for an additional 30 min. Afterward, mice received a KET injection (10 mg kg^{-1}; i.p.) by a male or female experimenter and were assessed for locomotor activity for 60 min. Distance traveled and time spent in the center of the open-field arena were analyzed using TopScan v.2.0 (CleverSys).

Western blots.

Male CD1 mice received a KET (10 mg kg^{-1}; i.p.) or vehicle injection by either male or female experimenters and were euthanized via cervical dislocation 24 h post-treatment. The ventral hippocampi were dissected and homogenized in Syn-PER Reagent (ThermoFisher Scientific; 87793) with 1 × protease and phosphatase inhibitor cocktail (ThermoFisher Scientific; 78440) to purify synaptoneurosomes. The homogenate was centrifuged for 10 min at 1,200*g* at 4 °C. The supernatant was then centrifuged again at 15,000*g* for 20 min at 4 °C. After centrifugation, the pellet consisting of the synaptosomal fraction was re-suspended and sonicated in N-PER Neuronal Protein Extraction Reagent (ThermoFisher Scientific; 87792). Protein concentration was determined using the BCA protein assay kit (ThermoFisher Scientific; 23227). Equal quantities of proteins (10–40 μg as optimal for each antibody) for each sample were loaded into NuPage 4–12% Bis-Tris gels for electrophoresis. Each gel contained one lane loaded with a size standard marker (BLUltra prestained protein ladder from Bio-Helix; cat. no. PM001-0500). Gel transfer was performed with the TransBlot Turbo Transfer System (Bio-Rad) nitrocellulose membranes. Membranes were blocked with 5% milk in TBST (0.1% Tween-20 in 1 × TBS) for 1 h and incubated with primary antibodies overnight at 4 °C. The following primary antibodies were used: GluA1 (Cell Signaling Technology; 185, Clone D4N9V, Lot 3; dilution 1:1,000) and GAPDH (Abcam; ab8245, Clone 6C5, Lot GR3275542-1; dilution 1:10,000). The next day, blots were washed three times in TBST and incubated with horseradish peroxidase-conjugated anti-mouse (GE Healthcare; cat. no. NV931V, Lot 16715063; dilution 1:10,000)

or anti-rabbit secondary antibody (Millipore; cat. no. AP182P, Lot 3766659; dilution 1:5,000) for 1 h. After three final washes with TBST, bands were detected using enhanced chemiluminescence with the Syngene Imaging System (G:Box ChemiXX9). Other sections of the blot were incubated with the primary antibody directed against GAPDH for loading control. Densitometric analysis of immunoreactive bands for each protein was conducted using Syngene's GenTools software. Protein levels were normalized to GAPDH. Fold change was calculated by normalization to the SAL-treated control group.

Brain levels of KET and metabolites.

Male CD1 mice received a KET (10 mg kg^{-1}; i.p.) injection by either a male or female experimenter and were decapitated at 10, 30, 60 or 240 min postinjection following a 2-min exposure to 3% isoflurane. Whole brains were collected and immediately frozen on dry ice, and stored at −80 °C until use. Experiments were performed by three pairs of experimenters.. The euthanasia and sample collection were conducted by the same experimenter who performed the injections. Three separate cohorts were performed with three different pairs of experimenters.

Achiral liquid chromatography–tandem mass spectrometry was used to determine the concentrations of KET and its metabolites in brain tissue as previously described[8]. Brains were suspended in 990 μl of water:methanol (3:2, v/v) with the addition of D_4-KET (10 μl of 10 μg ml^{-1}). The subsequent mixture was homogenized on ice with a polytron homogenizer and centrifuged at 21,000*g* for 30 min. The supernatant was processed using 1-ml Oasis HLB solid-phase extraction cartridges (Waters), which were previously pre-conditioned with 1 ml of methanol, followed by 1 ml of water and then 1 ml of ammonium acetate (10 mM, pH 9.5). Following the addition of the supernatants to the cartridges, 1 ml of water was added and the compounds were eluted with 1 ml of methanol. The eluent was transferred to an autosampler vial for analysis. Quality control standards were prepared at 200, 500 and 1,000 ng ml^{-1}. The quantification of (*R,S*)-KET, (*R,S*)-norketamine and HNK was accomplished by calculating area ratios using D_4-KET (10 μl of 10 μg ml^{-1} solution) as the internal standard. Area under the curve (AUC) was calculated using GraphPad Prism v.9.

qEEG.

qEEG experiments were performed according to previously published methods[8,13] with minor modifications. Mice were anesthetized with isoflurane, as described above. Analgesia was provided to the mice (carprofen, 5 mg kg^{-1}; s.c.) before the start of surgery. An ETA-F10 radio-telemetric transmitter (Data Sciences International) was placed subcutaneously and its leads implanted over the dura above the frontal cortex (1.7 mm anterior to bregma) and the cerebellum (6.4 mm posterior to bregma). Surgeries were performed by either female or male experimenters. Animals were allowed to recover for 7 d before recordings. Mice were single-housed and placed in the behavioral room immediately after the surgeries. qEEGs were recorded using the Dataquest A.R.T. 4.3 and Ponemah v.6.32 acquisition systems (Data Sciences International) with frontal qEEG recordings referenced to the cerebellum.

Male and female experimenters injected KET (10 mg kg^{-1}; i.p.) interchangeably with a 30-min gap time between the male experimenter injections and the female experimenter injections. Before KET administration, baseline (pre-injection) recordings were analyzed for 30 min previously for each experimenter. An additional 60-min analysis was performed following KET injection.

qEEGs were analyzed using Neuroscore v.3.2.9297-1 (DSI). An automated analysis protocol was implemented to mark occurrences of invalid signal data/artifacts. These artifacts were defined using an amplitude detector set at greater than or equal to an absolute threshold of 0.001 mV, with a minimum duration of 10 μs, maximum duration of 10 s, joint interval of 1 s, prepend duration of 0.01 s and append duration of 0 s. qEEG signals were exported as periodograms using the following parameters: values to 6 decimal places using 10-s epochs, Hamming windows, a Fast Fourier Transform order of 10, 50% overlap and excluding epochs overlapping invalid data markers. These parameters yielded periodograms with frequency bins of 0.98 Hz. Oscillation power in each bandwidth (delta = 1–3 Hz; theta = 4–7 Hz; alpha = 8–12 Hz; beta = 13–29 Hz; gamma = 30–100; high frequency oscillations (HFO): 100–160 Hz) was calculated in 10-min bins.

Spectrograms expressed in log scales and represented as heat maps were created in MATLAB 2018a by generating average periodograms within treatment groups and normalizing over mean treatment group baseline values for each frequency bin. Average power changes across frequencies were calculated in MATLAB by dividing power values averaged across 30 min post-treatment by power values averaged across the baseline for each animal in each frequency bin. Graphs of mean and s.e.m. were generated using GraphPad Prism v.8.3.

fEPSPs.

Mice were euthanized by a brief exposure to 3% isoflurane, followed by decapitation. Removal of the mouse brains and extraction of the hippocampi were performed in ice-cold ACSF bubbled with 95% O_2 and 5% CO_2. The ACSF contained (in mM): 124 NaCl, 3 KCl, 1.25 NaH_2PO_4, 1.5 $MgCl_2$, 2.5 $CaCl_2$, 26 $NaHCO_3$ and 10 glucose. Hippocampal slices were cut at 400 μm using a vibratome and kept in a holding chamber at the interface of air–ACSF and humidified 95% O_2, 5% CO_2 for at least 1 h. For the fEPSPs, slices were transferred to a submersion-type recording chamber and perfused with ACSF (0.5–2 ml min^{-1}; room temperature (RT)). Concentric bipolar tungsten electrodes were placed in stratum radiatum to stimulate the SC afferents or in the stratum lacunosum-moleculare to stimulate EC afferents. Extracellular recording pipettes were filled with ACSF (3–5 MΩ) and placed in stratum radiatum for the SC or in the stratum lacunosum-moleculare for the EC–CA1 pathway stimulation. Field potentials were evoked by 100-μs pulses delivered at 0.1 Hz. Baseline stimulus strength was set to ~40–50% of the maximum field potential response to facilitate observing an increase in excitability and to avoid a possible ceiling effect. A stable baseline was recorded for at least 10 min. Vehicle, CRF (125 nM) and (*2R,6R*)-HNK (3 or 15 μM) were applied by superfusion over a period of 1 h. For AMPAR-mediated responses, peak fEPSP slopes, measured over a window of 1–4 ms following the rising phase of the response, were reported as percentage change from baseline. DNQX (50

μM) was bath-applied at the end of the recording to confirm AMPAR-mediated responses. Treatments were randomly assigned before the beginning of the recordings; however, the experimenter was not blind to the treatment groups during the experiment. Analysis of the fEPSPs was performed by an experimenter blind to the treatment groups. Experiments were performed using pCLAMP software v.10 (Molecular Devices). Calculations of the fEPSP slopes were performed with Clampfit v.11.0.3 (Molecular Devices). Statistical analysis for the potentiation experiments was performed using the average of the last 5 min of the wash-in period. In the experiment in which CP-154,526 was used, comparisons were performed between the average of the last 5 min of the pre-wash-in and the last 5 min of the wash-in period.

Whole-cell slice electrophysiology.

Heterozygous CRF-ires-cre mice that previously received a 300-nl injection of AAV5.EF1a-DIO-eYFP-WPRE-hGH or AAV5.EF1a-DIO-hChR2(H134R)-eYFP-WPRE-hGH (Penn Vector Core and Addgene) into the EC (AP: −2.8, ML: ±4.25, DV: −5.17 from the top of the skull) at a rate of 20 nl min^{-1} using a 1-μl Hamilton syringe (Knurled Hub Needle, 25 G) were used. Five weeks following injections, mice were decapitated. Their brains were rapidly removed and transferred to an oxygenated (95% O_2, 5% CO_2) ice-cold solution containing (in mM): 30 NaCl, 2.5 KCl, 1.25 NaH_2PO_4, 26 $NaHCO_3$, 10 $MgCl_2$, 0.5 $CaCl_2$, 10 glucose 230 sucrose. Then, 250-μm-thick coronal slices containing the hippocampus were sectioned using a Leica VT1200S vibratome (Leica Biosystems) and transferred to a holding chamber filled with oxygenated solution containing (in mM): 109 NaCl, 4.5 KCl, 1.2 NaH_2PO_4, 35 $NaHCO_3$, 1 $MgCl_2$, 2.5 $CaCl_2$, 11 glucose, 20 HEPES, 0.4 ascorbic acid. Slices were left at RT in the holding chamber for at least 1 h before the start of the experiments. Afterward, slices were transferred to a small-volume (<0.5 ml) recording chamber that was mounted on a fixed-stage upright microscope (Nikon Eclipse E600FN) equipped with differential interference contrast optics and immersed in oxygenated ACSF containing (in mM): 125 NaCl, 2.5 KCl, 1.25 NaH_2PO_4, 26 $NaHCO_3$, 1.5 $MgCl_2$, 2.4 $CaCl_2$, 25 glucose. All solutions had pH of 7.4 and about 310 mOsm. Experiments were performed at RT and the ACSF was flowing at 2 ml min^{-1}. Neuronal soma was visualized at high magnification (×40, 0.8 NA water-immersion objective; Nikon). Conventional tight-seal (>2 GΩ) whole-cell patch-clamp recordings were acquired using a Multiclamp 700B (Molecular Devices) amplifier from CA1 stratum lacunosum moleculare (SLM) interneurons voltage clamped at −60 mV. Signals were filtered at 1 kHz and digitized at 10 kHz using Axon Digidata 1550B (Molecular Devices). Recording pipettes (3.5–5 MΩ) were pulled with a P-97 horizontal micropipette puller (Sutter Instruments) filled with internal solution containing (in mM): 100 $CsCH_3SO_3$, 50 CsCl, 10 HEPES, 2 $MgCl_2$, 0.2 EGTA, 10 phosphocreatine (Tris), 4 Mg-ATP, 0.3 Na-GTP. On the day of the experiment, 1.5 mg ml^{-1} QX-314 was added to the internal solution (pH was adjusted to 7.2–7.3 with CsOH, osmotic concentration adjusted to 285–290 mOsm). Neurons were filled with biocytin (5 mg ml^{-1}) for post-experimental identification. PSCs were evoked using optical stimulation (473 nm; 4–6 ms; 6–7 mW) every 60 s, for 15 min. DNQX (25 μM) and DL-AP5 (50 μM) were bath-applied to block AMPA and NMDA receptors. After 10 min of drug application, PSCs were evoked using the same procedure for another 15 min. Stimulation protocols were generated and signals were acquired using Clampex 11.2 software (Molecular Devices).

Series resistance was monitored and the data were discarded if the resistance increased over 20% during recordings. Data were analyzed using WinWCP v.5.3.3 software (courtesy of Dr. John Dempster, Strathclyde University, Glasgow, UK).

Anatomical tracing.

Heterozygous CRF-ires-cre mice received a 200-nl injection of AAV pCAG-FLEX-tdTomato-WPRE virus and wild-type mice received 1% CTb at a rate of 20 nl min^{-1} using a 1-μl Hamilton syringe (Knurled Hub Needle, 25 G) in the ventral CA1 (AP: −2; ML: ±3.5; DV: −4.5 from the top of the skull). Four weeks after the injections, mice were perfused with 4% paraformaldehyde (PFA) transcardially; their brains were extracted and stored in 4% PFA at 4 °C for at least 24 h before sectioning with a vibratome (50-μm thickness). For the CTb mice, brains were fresh-frozen and processed for RNAscope as described below.

RNAscope for CRF and Fos.

We utilized RNAscope Fluorescent Multiplex Detection Reagent Kit (ACDbio; 320851) according to the manufacturer's instructions. Mice were euthanized via cervical dislocation 30 min following exposure to cotton-tipped swabs containing either male or female experimenters' scent. Brains were extracted, frozen in chilled isopentane and stored at −80 °C. Fresh-frozen brain sections (20 μm) were collected using a cryostat (Leica CM1900) and directly mounted onto charged slides. Slides were fixed in 4% PFA in 1 × PBS, dehydrated in increasing concentrations of ethanol (50%, 70%, 100%, 100%), air-dried and outlined with a hydrophobic barrier pen. Slides then underwent Protease Plus treatment for 5 min, followed by two 1 × PBS washes for 2 min each. Sections were hybridized with RNAscope probes against *CRH* (ACDbio: 316091-C1) and *Fos* (ACDbio: 316921-C2) for 2 h at 40 °C, followed by two washes in 1 × RNAscope Washing Buffer, 2 min each. After hybridization, sections were incubated with AMP1 (30 min), AMP2 (15 min), AMP3 (30 min) and AMP4A (15 min) sequentially, with two washes in 1 × RNAscope Washing Buffer (2 min each) at RT in between each step. Lastly, sections were incubated in DAPI for 1 min at RT, rinsed, coverslipped with Vectashield Vibrance antifade mounting medium (Vector Laboratories) and allowed to set overnight at 4 °C before imaging. Analysis of RNAscope was performed by the automated image analysis software Imaris v.9.2.1 (Oxford Instruments). For the analysis of CRF and Fos, a positive cell was defined as one that expressed ≥5 CRF transcripts and ≥3 Fos transcripts simultaneously. For the colocalization analysis, a positive cell was defined as one that expressed ≥5 CRF transcripts and ≥3 Fos transcripts. Results from Imaris were validated via manual counting by an experimenter blind to the experimental groups.

In vivo fiber photometry.

Heterozygous CRF-ires-cre mice received 250-nl bilateral infusions of retrograde AAV-syn-FLEX-jGCaMP7s-WPRE (AP: −2.3; ML: ±3.25; DV: −4.8 from top of the skull) in the ventral CA1. At 3–4 weeks after the virus infusion, mice were bilaterally implanted with fiber optic cannulas (200 μm, 0.37 NA) in the EC. Following a minimum of 10-d recovery, mice were exposed to the male, female and control scents in the Y-maze equipment. Each arm was 11.4 cm long, with a metal barrier at the end of the arm to fit the tip of the swab. Mice were habituated in the equipment for 8 min followed

by 8 min of testing; swabs were inserted into each arm at the beginning of each testing session. During the habituation and testing phases, mice were connected to the fiber photometry system (Neurophotometrics) to record calcium transients from CRF-expressing EC neurons that project to the CA1 using a low-autofluorescence bifurcated optic patch cable (Doric Lenses). An entry event was counted when all four paws of the mouse crossed to another arm. Independence of signals was tested before the start of the experiment. Excitation wavelengths used were 470 nm for the calcium-dependent rjGCaMP7s signal and temporally interleaved with 410-nm light at 40 Hz for the calcium-independent (isosbestic) signal. During the test period, photometry data were recorded and timestamped using Bonsai as published by Neurophotemetrics. The code is available at the company website (https://static1.squarespace.com/static/60ff345fca665d50e1adc805/t/616103731b92d50b0f4d5833/1633747831997/Full+Length+Manual-2021.pdf). The fiber photometry data were analyzed offline and corrected for photobleaching using pMAT v.1.2 (ref. [41]); the 410-nm signal was scaled and fitted to the 470-nm signal before subtraction to correct for any motion artifacts. The z-score was calculated for the peri-event trial, which was defined as the 5 s before the entrance into each arm and 10 s after the entrance. The signals for all the trials were averaged for each animal. Following the calculation of z-scores, a smoothing filter was applied to eliminate high-frequency noise, and AUC was calculated. The AUC was calculated using GraphPad v.9. For the calculation the trapezoid method was used and the mean curves of the replicated values were used, thus yielding one value. For the calculation of the s.e.m. and confidence intervals for the AUC, the method described by Gagnon and Peterson[42] was used. This assumes that each animal is a replicate measurement in one experiment, which yields one value per group. As such, each animal serves as a replication rather than as a completely new experiment. Each mouse was exposed to a different experimenter scent and the location of the swabs was counterbalanced.

Statistical analysis.

Details of all *n* numbers, statistical analyses, effect sizes and results are provided in Supplementary Tables 1 and 2. Required sample sizes were estimated based on our past experience performing similar experiments. Animals were not excluded from the analysis except for medical reasons. For viral injection experiments animals were excluded if the injection was not in the correct region or there was no expression. For cannula implantation experiments animals were excluded if the implantation of the cannula was not in the correct region. All statistical tests were two-tailed and significance was set at $P < 0.05$. Data were tested for equal variance and Gaussian distribution using the Brown–Forsythe test and Kolmogorov–Smirnov test, respectively. When normality and equal variance were achieved, parametric statistical tests were performed. Correction for multiple comparisons for data analyzed with parametric analyses of variance (ANOVAs) was performed using the Holm–Sidak post-hoc test. When normality and/or equal variance of samples failed, nonparametric tests were used. Correction for multiple comparisons for data analyzed with the nonparametric Kruskal–Wallis test was performed using the two-stage linear step-up procedure of Benjamini, Krieger and Yekutieli. Nonlinear regression curve fit was used to plot the RNAscope results using the one-phase exponential decay model followed by the extra-sum-of-squares test. Effect sizes were calculated by Cohen's *D* test. For analysis of the ROC graphs we compared the AUC. Statistical analyses were performed using GraphPad

Prism v.9 except for the Wilcoxon matched-pairs signed-rank tests, which were performed using SigmaPlot v.14.0.

Extended Data

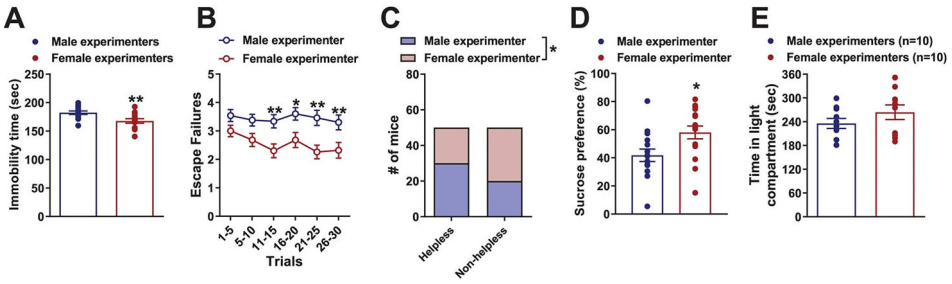

Extended Data Fig. 1 |. Sex of human experimenter effects on stress-related behaviours. (**a**) Immobility time measured in the forced-swim test (FST) following saline injections by male and female experimenters in CD1 mice combined from all the experiments performed for the present manuscript where the mean immobility time of each experiment was used (n = 13 experiments; two-sided unpaired *t*-test, p = 0.007). (**b,c**) Escape failures following inescapable shock training in the learned helplessness paradigm in Swiss-Webster (CFW) mice handled by a male or a female experimenter (n = 50 mice; two-sided Kruskal-Wallis followed by correction with two-stage linear step-up procedure of Benjamini, Krieger and Yekutieli for B; 11–15 trials q = 0.0099, 16–20 trials q = 0.021, 21–25 trials q = 0.004, 26-30 trials q = 0.0125 and two-sided chi-square test for C, p = 0.046). (**d**) Average sucrose preference over 48 hours following 10-days of chronic social defeat performed by a male and female experimenter (C57BL/6 J mice; $n = 15$, 16 mice; two-sided unpaired *t*-test; p = 0.016) and (**e**) time spent in light compartment in the light/dark box performed by male and female experimenters (CD1 mice; n = 10 experimenters; n = 20 mice/sex; two-sided unpaired *t*-test; p = 0.221). Data shown are mean ± S.E.M. * $p < 0.05$; ** $p < 0.01$. For detailed statistics information, see Supplementary Table 1.

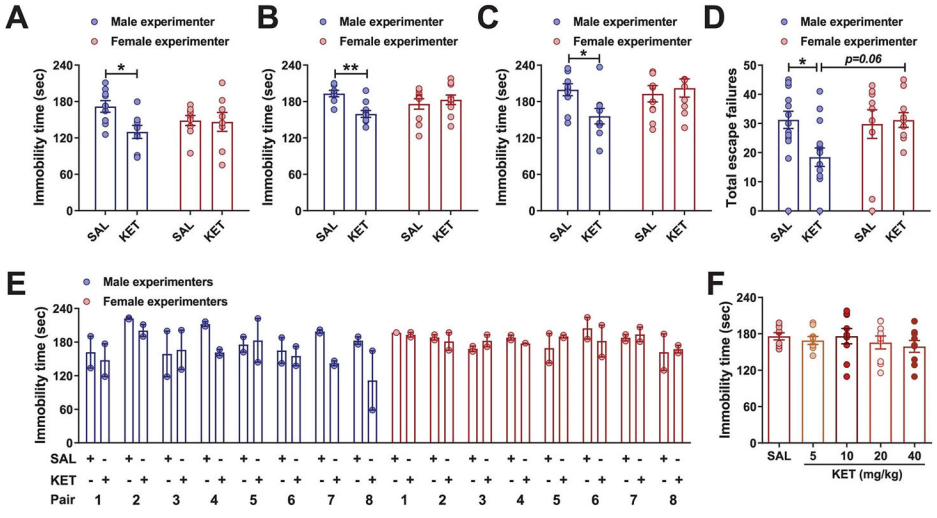

Extended Data Fig. 2 |. Effects of the sex of human experimenter on the antidepressant responses to ketamine.

(**a**) Immobility time in the forced-swim test (FST) 24 hours post- saline (SAL; 7.5 ml/kg) and ketamine (KET; 10 mg/kg) injections by a male and female experimenter in male CD1 mice (n = 9,8,9,8 mice; two-sided two-way ANOVA followed by |Holm-Sidak test; p = 0.023). (**b**) Immobility time in the FST 1-hour post-SAL or KET (10 mg/kg) injection by a male or female experimenter in female CD1 mice (n = 10 mice/experimenter/treatment group; two-sided Kruskal-Wallis followed by correction with two-stage linear step-up procedure of Benjamini, Krieger and Yekutieli; q = 0.0096). (**c**) Immobility time 1-hour post-SAL (7.5 ml/kg) or KET (10 mg/kg) injection by a male or female experimenter in male CD1 mice pre-exposed to a 15-min swim session 24 hours prior to the FST (n = 10,9,10,9 mice; two-sided two-way ANOVA followed by |Holm-Sidak test; p = 0.024). (**d**) Total escape failures in the learned helplessness paradigm following SAL (7.5 ml/kg) or KET (10 mg/kg) injections by male and female experimenters in male Swiss-webster (CFW) mice (n = 16,14,10,10 mice; two-sided two-way ANOVA followed by |Holm-Sidak test; p = 0.032). (**e**) Immobility scores in the FST 1-hour following SAL (7.5 ml/kg) or KET (10 mg/kg) injections for each individual experimenter in male CD1 mice, performed at a different institution (n = 2/experimenter). (**f**) KET dose-response (5, 10, 20, 40 mg/kg) in the FST 1-hr post-injection by a female experimenter in male CD1 mice (n = 9 mice/dose; two-sided one-way ANOVA). Data are shown as mean ± S.E.M. * $p < 0.05$, ** $p < 0.01$. For detailed statistics information, see Supplementary Table 1.

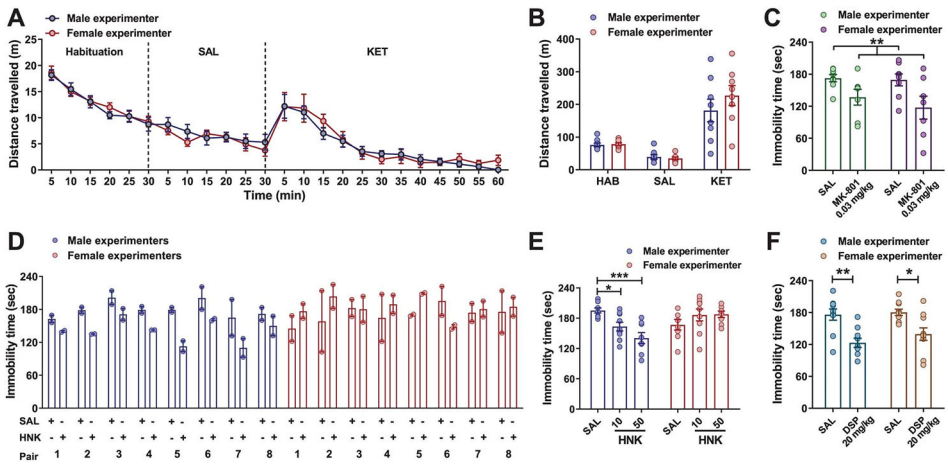

Extended Data Fig. 3 |. Sex of human experimenter effects on NMDAR inhibition dependent behavioural effects.

Distance travelled per 5 min binned intervals in the open-field test in male CD1 mice that received no treatment (HAB; habituation) followed by injections of saline (SAL; 7.5 ml/kg) and then ketamine (KET; 10 mg/kg) administered by a male or female experimenter (n = 8 mice/experimenter/treatment group; two-sided RM two-way ANOVA with Geisser-Greenhouse correction). Immobility time in the forced-swim test 1-hour post-injection following administration of the (**c**) N-methyl-D-aspartate (NMDAR) receptor antagonist, MK-801 (0.03 mg/kg) (CD1 mice; n = 8,7,8,7 mice; two-sided two-way ANOVA; Treatment effect: p = 0.004), (**d,e**) ketamine metabolite, (*2R,6R*)-hydroxynorketamine (HNK; 10 and 50 mg/kg; CD1 mice; n = 2/experimenter for D and; n = 8,9,8,8,9,8 mice and two-sided

two-way ANOVA followed by Holm-Sidak test for E; SAL vs 10 mg/k – p = 0.038, SAL vs 50 mg/kg – p = 0.0006), and (**f**) the classical antidepressant desipramine (DSP; 20 mg/kg) vs SAL (7.5 ml/kg) injections by a male or female experimenters (CD1 mice; $n = 10$ mice/group; two-sided Kruskal-Wallis followed by correction with two-stage linear step-up procedure of Benjamini, Krieger and Yekutieli; Male: p = 0.001, Female: p = 0.011). Data are shown as mean ± S.E.M. * $p < 0.05$; ** $p < 0.01$; *** $p < 0.001$. For detailed statistics information, see Supplementary Table 1.

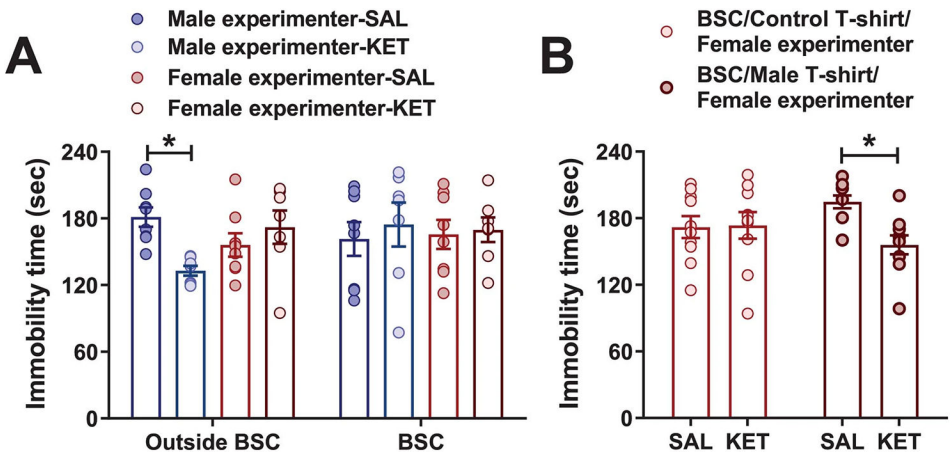

Extended Data Fig. 4 |. Effects of experimenter scent on the antidepressant-like responses of ketamine.

(**a**) Elimination of experimenter scent by administering saline (SAL; 7.5 ml/kg) or ketamine (KET; 10 mg/kg) within a biosafety cabinet and testing the mice in the forced-swim test (FST) 1-hour post-injection (CD1 mice; n = 8,7,8,7,8,7,8,7 mice; two-sided three-way ANOVA followed by Holm-Sidak test; p = 0.043). (**b**) Immobility time in mice tested in the FST 1-hour following injections of SAL (7.5 ml/kg) and KET (10 mg/kg) performed on a male worn t-shirt within the biosafety cabinet by a female experimenter (CD1 mice; $n = 10$ mice/group; two-sided two-way ANOVA followed by Holm-Sidak test; p = 0.011) Data are shown as mean ± S.E.M. * $p < 0.05$. For detailed statistics information, see Supplementary Table 1.

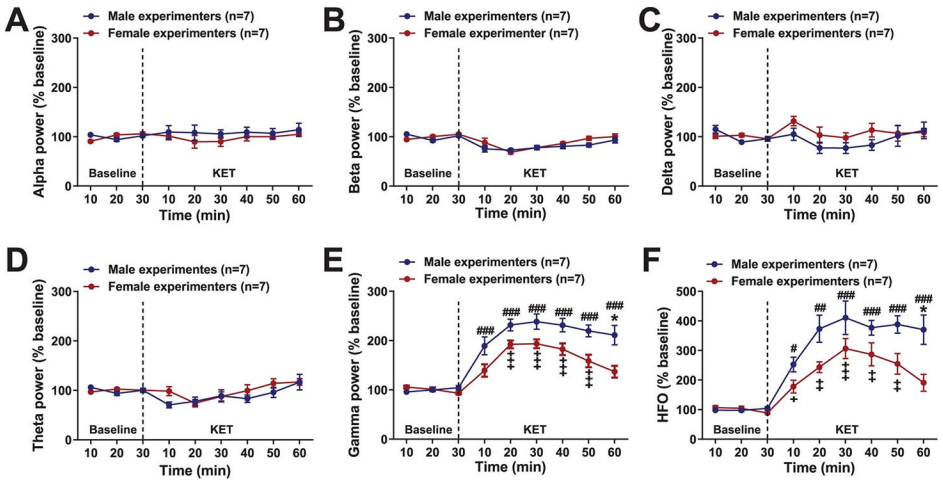

Extended Data Fig. 5 |. Effects of experimenter scent on the quantitative electroencephalographic oscillations.

Effects of ketamine (KET; 10 mg/kg) administration by male and female experimenters on cortical quantitative electroencephalographic (qEEG) measurements in CD1 mice (n = 7 experimenters; n = 28–29 mice/sex) using the traditionally defined frequency bands (**a**) alpha (8–12 Hz), (**b**) beta (13–29 Hz), (**c**) delta (1–4 Hz), (**d**) theta (4–8 Hz), (**e**) gamma (30–100 Hz; two-sided Kruskal-Wallis followed by correction with two-stage linear step-up procedure of Benjamini, Krieger and Yekutieli; Male: Baseline vs 10 q = 0.0121, vs 20 q = 0.0003, vs 30 q = 0.0003, vs 40 q = 0.0005, vs 50 q = 0.0009, vs 60 q = 0.0022; Female: Baseline vs 10 q = 0.057, vs 20 q = 0.0011, vs 30 q = 0.0009, vs 40 q = 0.0023, vs 50 q = 0.0124, vs 60 q = 0.0613; Male vs Female q = 0.0426), and (**f**) high frequency oscillations (100–160 Hz; two-sided Kruskal-Wallis followed by correction with two-stage linear step-up procedure of Benjamini, Krieger and Yekutieli; Male: Baseline vs 10 q = 0.0315, vs 20 q = 0.0011, vs 30 q = 0.0004, vs 40 q = 0.0004, vs 50 p = 0.0004, vs 60 q = 0.0013; Female: Baseline vs 10 q = 0.0446, vs 20 q = 0.0074, vs 30 q = 0.0004, vs 40 q = 0.0011, vs 50 q = 0.0039, vs 60 p = 0.0539; Male vs Female p = 0.0342). Data are normalised to baseline, and the dashed vertical line indicates the time point of ketamine administration. Data are shown as mean ± S.E.M. $^{+}$, $^{\#}$ $p < 0.05$; $^{++}$, $^{\#\#}$ $p < 0.01$; $^{+++}$, $^{\#\#\#}$ $p < 0.001$. Differences between ketamine response administered by male and female experimenters is indicated by *. Differences between baseline and ketamine is indicated by # for male experimenters and by + for female experimenters. For detailed statistics information, see Supplementary Table 1.

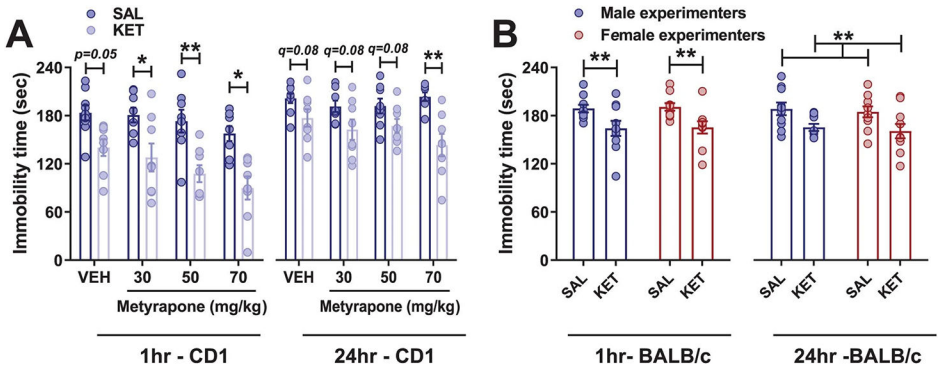

Extended Data Fig. 6 |. Effects of corticosterone on the antidepressant responses to ketamine.

(**a**) Forced-swim test (FST) immobility measured in mice that received metyrapone (30, 50 and 70 mg/kg) prior to KET (10 mg/kg) and tested 1- and 24-hours later (CD1 mice; n = 9,8,8,8,8,8,8,8 mice; two-sided Kruskal-Wallis followed by correction with two-stage linear step-up procedure of Benjamini, Krieger and Yekutieli; VEH-SAL vs VEK-KET p = 0.028, MET 30-SAL vs MET 30-KET p = 0.028, MET 50-SAL vs MET 50-KET p = 0.009, MET 70-SAL vs MET 70-KET p = 0.019 for 1 -hour; MET 70-SAL vs MET 70-KET p = 0.0021 for 24-hours). (**b**) Immobility time measured in the FST following saline (SAL; 7.5 ml/kg) or ketamine (KET; 10 mg/kg) administration by male and female experimenters to male BALB/cAnNCrl mice (n = 10 mice/treatment group; two-sided Kruskal-Wallis followed by correction with two-stage linear step-up procedure of Benjamini, Krieger and Yekutieli for 1-hour; Male: SAL vs KET q = 0.0075, Female: SAL vs KET q = 0.0069 and two-sided two-way ANOVA for 24-hours; Treatment effect: p = 0.0024). Data are shown as mean ± S.E.M. * $p < 0.05$; ** $p < 0.01$; for non-parametric analysis ** $q < 0.01$. For detailed statistics information, see Supplementary Table 1.

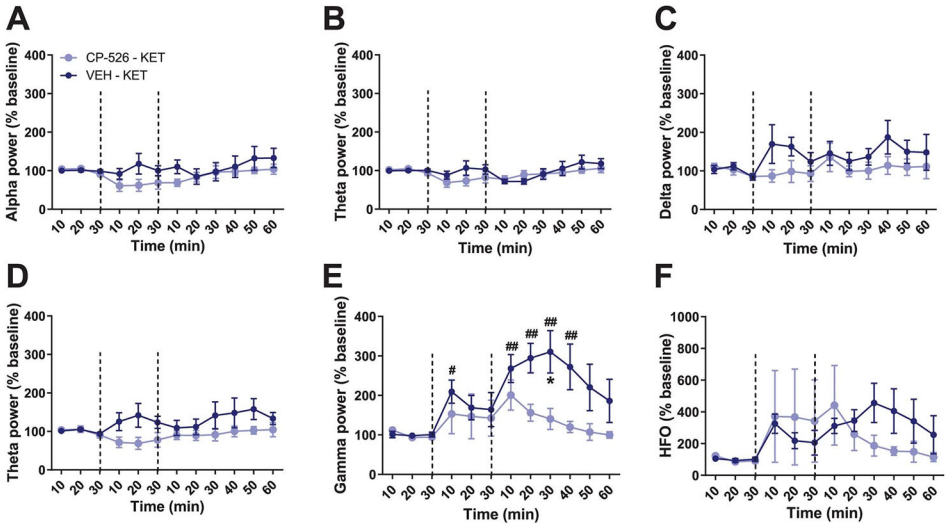

Extended Data Fig. 7 |. Effects of the CRF1 antagonist, CP-154,526, on electroencephalographic measures following ketamine administration.

Effects of the corticotropin-releasing factor 1 antagonist (CRF1), CP-154,526 (CP-526; 30 mg/kg) or vehicle (VEH; 1.5 ml/kg) prior to ketamine (KET; 10 mg/kg) administration by a

male experimenter on cortical qEEG measurements in CD1 mice (n = 6 mice/treatment group) using the traditionally defined frequency bands (**a**) alpha (8–12 Hz), (**b**) beta (13–29 Hz), (**c**) delta (1–3 Hz), (**d**) theta power (4–8 Hz), (**e**) gamma (30–100 Hz; two-sided Kruskal-Wallis followed by correction with two-stage linear step-up procedure of Benjamini, Krieger and Yekutieli (pre-selected comparisons); VEH-KET vs CP-526-KET at 30 min q = 0.0439 and at 40 min q = 0.0518; Baseline 30 min vs 10 min VEH q = 0.0407, vs 10 min KET q = 0.0086, vs 20 min KET q = 0.0068, vs 30 min KET q = 0.0068, vs 40 min KET q = 0.0094, vs 50 min KET q = 0.052, vs 60 min KET q = 0.1150), and (**f**) high frequency oscillations (100–160 Hz). Data are normalised to baseline. The first dashed vertical line indicates the time point of VEH or CP-526 administration and the second dashed vertical line indicates the time point of KET administration. Data are shown as mean ± S.E.M. *, # $p < 0.05$, ***, ### $p < 0.001$. Differences between mice pre-treated with CP-526 and VEH are indicated by *. Differences between the baseline and treatment in mice that received VEH prior to KET are indicated with #. For detailed statistics information, see Supplementary Table 1.

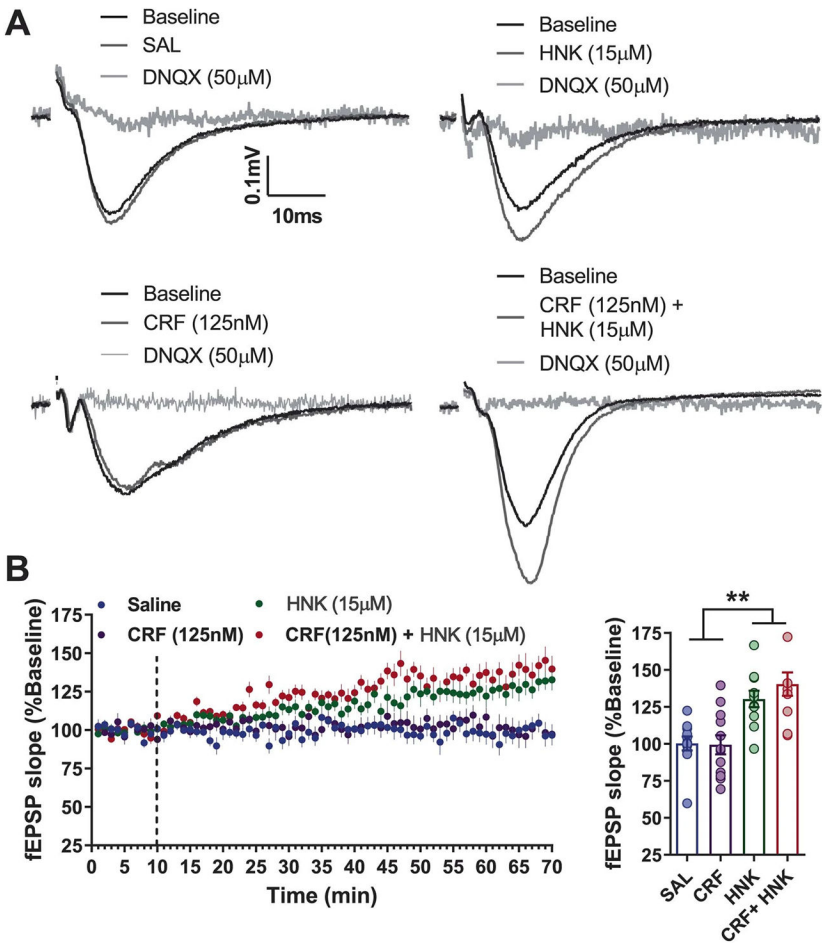

Extended Data Fig. 8 |. Effects of the combined CRF and (*2R,6R*)-hydroxynorketamine on field excitatory postsynaptic potentials in hippocampal slices in the SC-CA1 pathway.

(**a**) Representative traces of Schaffer collateral-hippocampal CA1 (SC-CA1) field excitatory postsynaptic potentials (fEPSPs) and (**b**) quantification of fEPSPs slopes following SC-CA1

pathway stimulation during wash-in with Saline (SAL; n = 11 slices), corticotropin-releasing factor (CRF; 125 nM; n = 12 slices), (*2R,6R*)-hydroxynorketamine (HNK; 15 μM; n = 11 slices) or combined CRF (125 nM) + (*2R,6R*)-HNK (15 μM) (n = 11 slices; two-sided one-way ANOVA followed by Holm-Sidak test; SAL vs HNK p = 0.0053, SAL vs CRF+ HNK p = 0.0003, CRF vs HNK p = 0.0043, CRF vs CRF + HNK p = 0.0002). Data are shown as mean ± S.E.M. ** $p < 0.01$. For detailed statistics information, see Supplementary Table 1.

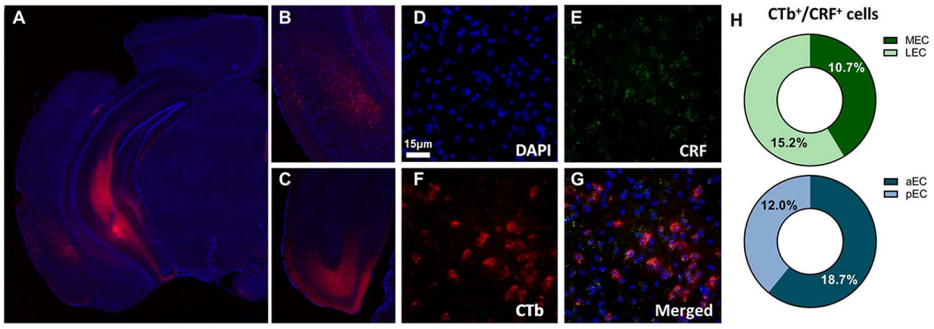

Extended Data Fig. 9 |. Identification of EC to CA1 projections.

(**a**) Representative images of the injection site at ventral CA1 with retrograde conjugated cholera toxin and the (**b,c**) labelling in the anterior and posterior entorhinal cortex (EC). Representative RNAscope images from the EC revealing (**d**) DAPI labeling, (**e**) CRF transcript labelling, (**f**) CTb labelling and (**g**) the co-labelling between the tracer and CRF transcripts. (**h**) Quantification of RNA scope and tracer co-labelling at the anterior (aEC) and posterior EC (pEC) and the lateral (LEC) and medial EC (MEC) (n = 8-9 samples from 2 animals thus these findings were independently replicated twice).

Supplementary Material

Refer to Web version on PubMed Central for supplementary material.

Acknowledgements

We thank D. Sparta for providing the CRF-ires-cre founder mice. We thank the many volunteers participating in these experiments. Brain section schematics were created with BioRender.com. This work was supported by NIH grant no. MH107615 and VA Merit grant no. 1I01BX004062 (T.D.G.), NIH grant no. MH086828 (S.M.T.) and NIH grant no. MH093897 (R.S.D.). R.M. and C.A.Z. laboratories are supported by the NIH Intramural Research Program. The contents do not represent the views of the US Department of Veterans Affairs or the US government.

Data availability

Data supporting the findings of this study are available within the paper and its Supplementary Information files. Source data are provided with this paper.

Code availability

Bonsai script was from the Neurophotometrics system manual at https://static1.squarespace.com/static/60ff345fca665d50e1adc805/t/616103731b92d50b0f4d5833/1633747831997/Full+Length+Manual-2021.pdf

References

1. Mogil JS Laboratory environmental factors and pain behavior: the relevance of unknown unknowns to reproducibility and translation. Lab Anim. 46, 136–141 (2017).
2. Sorge RE et al. Olfactory exposure to males, including men, causes stress and related analgesia in rodents. Nat. Methods 11, 629–632 (2014). [PubMed: 24776635]
3. Davis H, Taylor AA & Norris C Preference for familiar humans by rats. Psychon. Bull. Rev 4, 118–120 (1997).
4. van Driel KS & Talling JC Familiarity increases consistency in animal tests. Behav. Brain Res 159, 243–245 (2005). [PubMed: 15817187]
5. Can A et al. The mouse forced swim test. J. Vis. Exp (2012) 10.3791/3638
6. Planchez B, Surget A & Belzung C Animal models of major depression: drawbacks and challenges. J. Neural Transm 126, 1383–1408 (2019). [PubMed: 31584111]
7. Samuels BA & Hen R in Mood and Anxiety Related Phenotypes in Mice: Characterization Using Behavioral Tests, Vol. 2 (ed. Gould TD) Ch. XXX (Humana Press, 2011)..
8. Zanos P et al. NMDAR inhibition-independent antidepressant actions of ketamine metabolites. Nature 533, 481–486 (2016). [PubMed: 27144355]
9. Li N et al. mTOR-dependent synapse formation underlies the rapid antidepressant effects of NMDA antagonists. Science 329, 959–964 (2010). [PubMed: 20724638]
10. Autry AE et al. NMDA receptor blockade at rest triggers rapid behavioural antidepressant responses. Nature 475, 91–95 (2011). [PubMed: 21677641]
11. Maeng S et al. Cellular mechanisms underlying the antidepressant effects of ketamine: role of α-amino-3-hydroxy-5-methylisoxazole-4-propionic acid receptors. Biol. Psychiatry 63, 349–352 (2008). [PubMed: 17643398]
12. Highland JN, Zanos P, Georgiou P & Gould TD Group II metabotropic glutamate receptor blockade promotes stress resilience in mice. Neuropsychopharmacology 44, 1788–1796 (2019). [PubMed: 30939596]
13. Zanos P et al. (2R,6R)-Hydroxynorketamine exerts mGlu 2 receptor-dependent antidepressant actions. Proc. Natl Acad. Sci. USA 116, 6441–6450 (2019). [PubMed: 30867285]
14. Zanos P et al. (R)-Ketamine exerts antidepressant actions partly via conversion to (2R,6R)-hydroxynorketamine, while causing adverse effects at sub-anaesthetic doses. Br. J. Pharmacol 176, 2573–2592 (2019). [PubMed: 30941749]
15. Lumsden EW et al. Antidepressant-relevant concentrations of the ketamine metabolite (2R,6R)-hydroxynorketamine do not block NMDA receptor function. Proc. Natl Acad. Sci. USA 116, 5160–5169 (2019). [PubMed: 30796190]
16. Kim J-W et al. Sustained effects of rapidly acting antidepressants require BDNF-dependent MeCP2 phosphorylation. Nat. Neurosci 24, 1100–1109 (2021). [PubMed: 34183865]
17. Wulf HA, Browne CA, Zarate CA & Lucki I Mediation of the behavioral effects of ketamine and (2R,6R)-hydroxynorketamine in mice by kappa opioid receptors. Psychopharmacology (Berl.) (2022) 10.1007/s00213-022-06118-4
18. Pham TH et al. Common neurotransmission recruited in (R,S)-ketamine and (2R,6R)-hydroxynorketamine-induced sustained antidepressant-like effects. Biol. Psychiatry 84, e3–e6 (2018). [PubMed: 29174592]
19. Chen BK et al. Sex-specific neurobiological actions of prophylactic (R,S)-ketamine, (2R,6R)-hydroxynorketamine, and (2S,6S)-hydroxynorketamine. Neuropsychopharmacology 45, 1545–1556 (2020). [PubMed: 32417852]
20. Zanos P et al. Ketamine and ketamine metabolite pharmacology: insights into therapeutic mechanisms. Pharmacol. Rev 70, 621 LP–621660 (2018). [PubMed: 29945898]
21. Yao N, Skiteva O, Zhang X, Svenningsson P & Chergui K Ketamine and its metabolite (2R,6R)-hydroxynorketamine induce lasting alterations in glutamatergic synaptic plasticity in the mesolimbic circuit. Mol. Psychiatry 23, 2066–2077 (2018). [PubMed: 29158578]
22. Aguilar-Valles A et al. Antidepressant actions of ketamine engage cell-specific translation via eIF4E. Nature 590, 315–319 (2021). [PubMed: 33328636]

23. Highland JN et al. Hydroxynorketamines: pharmacology and potential therapeutic applications. Pharmacol. Rev 73, 763 LP–763791 (2021). [PubMed: 33674359]
24. Fukumoto K et al. Activity-dependent brain-derived neurotrophic factor signaling is required for the antidepressant actions of (2R,6R)-hydroxynorketamine. Proc. Natl Acad. Sci. USA 116, 297–302 (2019). [PubMed: 30559184]
25. Carreno FR et al. Activation of a ventral hippocampus-medial prefrontal cortex pathway is both necessary and sufficient for an antidepressant response to ketamine. Mol. Psychiatry 21, 1298–1308 (2016). [PubMed: 26619811]
26. Hong LE et al. Gamma and delta neural oscillations and association with clinical symptoms under subanesthetic ketamine. Neuropsychopharmacology 35, 632–640 (2010). [PubMed: 19890262]
27. Smith SM & Vale WW The role of the hypothalamic-pituitary-adrenal axis in neuroendocrine responses to stress. Dialogues Clin. Neurosci 8, 383–395 (2006). [PubMed: 17290797]
28. Anisman H, Lacosta S, Kent P, McIntyre DC & Merali Z Stressor-induced corticotropin-releasing hormone, bombesin, ACTH and corticosterone variations in strains of mice differentially responsive to stressors. Stress 2, 209–220 (1998). [PubMed: 9787268]
29. Conti LH, Costello DG, Martin LA, White MF & Abreu ME Mouse strain differences in the behavioral effects of corticotropin-releasing factor (CRF) and the CRF antagonist α-helical CRF9-41. Pharmacol. Biochem. Behav 48, 497–503 (1994). [PubMed: 8090821]
30. Riggs LM et al. (2R,6R)-Hydroxynorketamine rapidly potentiates hippocampal glutamatergic transmission through a synapse-specific presynaptic mechanism.Neuropsychopharmacology 45, 426–436 (2020). [PubMed: 31216563]
31. Riggs LM, Thompson SM & Gould TD (2R,6R)-Hydroxynorketamine rapidly potentiates optically-evoked Schaffer collateral synaptic activity. Neuropharmacology 214, 109153 (2022). [PubMed: 35661657]
32. Blank T, Nijholt I, Eckart K & Spiess J Priming of long-term potentiation in mouse hippocampus by corticotropin-releasing factor and acute stress: implications for hippocampus-dependent learning. J. Neurosci 22, 3788–3794 (2002). [PubMed: 11978854]
33. Aldenhoff JB, Gruol DL, Rivier J, Vale W & Siggins GR Corticotropin releasing factor decreases postburst hyperpolarizations and excites hippocampal neurons. Science 221, 875–877 (1983). [PubMed: 6603658]
34. Wilson DA et al. Cortical odor processing in health and disease. Prog. Brain Res 208, 275–305 (2014). [PubMed: 24767487]
35. Bitzenhofer SH, Westeinde EA, Zhang H-XB & Isaacson JS Rapid odor processing by layer 2 subcircuits in lateral entorhinal cortex. eLife 11, e75065 (2022). [PubMed: 35129439]
36. Ferry B, Herbeaux K, Javelot H & Majchrzak M The entorhinal cortex is involved in conditioned odor and context aversions. Front. Neurosci 9, 342 (2015). [PubMed: 26483624]
37. Xu W & Wilson DA Odor-evoked activity in the mouse lateral entorhinal cortex. Neuroscience 223, 12–20 (2012). [PubMed: 22871522]
38. Persson BM et al. Lateral entorhinal cortex lesions impair odor-context associative memory in male rats. J. Neurosci. Res 100, 1030–1046 (2022). [PubMed: 35187710]
39. Butler-Struben HM, Kentner AC & Trainor BC What's wrong with my experiment?: The impact of hidden variables on neuropsychopharmacology research. Neuropsychopharmacology (2022) 10.1038/s41386-022-01309-1
40. McBride K, Slotnick B & Margolis FL Does intranasal application of zinc sulfate produce anosmia in the mouse? An olfactometric and anatomical study. Chem. Senses 28, 659–670 (2003). [PubMed: 14627534]
41. Bruno CA et al. pMAT: an open-source software suite for the analysis of fiber photometry data. Pharmacol. Biochem. Behav 201, 173093 (2021). [PubMed: 33385438]
42. Gagnon RC & Peterson JJ Estimation of confidence intervals for area under the curve from destructively obtained pharmacokinetic data. J. Pharmacokinet. Biopharm 26, 87–102 (1998). [PubMed: 9773394]

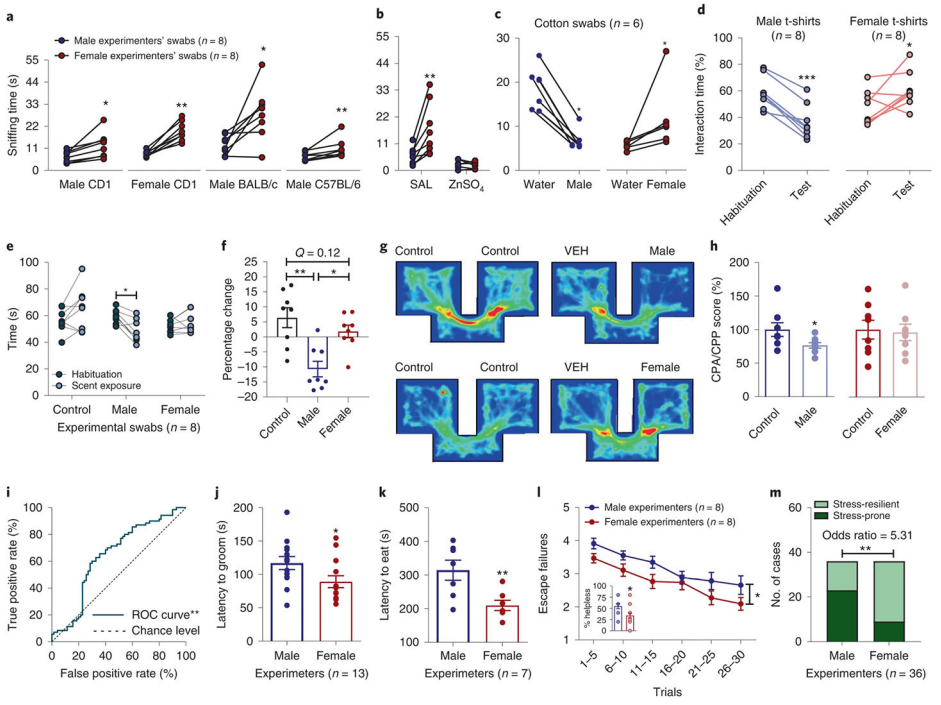

Fig. 1 |. Mice manifest differential behavioral responses following exposure to male and female experimenter scent.

a,b, Interaction time of experimentally naïve CD1 ($P = 0.010$ males, $P = 0.008$ females), BALB/cAnNCrl ($P = 0.016$), C57BL/6J ($P = 0.008$) ($n = 8$ experimenters per strain per sex; $n = 32$ mice per strain; two-sided paired *t*-test or Wilcoxon matched-pairs signed-rank test) (**a**) and anosmic CD1 mice with male versus female experimenter skin swabs ($n = 8$ experimenters per treatment group per sex; $n = 16$ mice per treatment group; two-sided Wilcoxon matched-pairs signed-rank test; SAL $P = 0.008$, $ZnSO_4$ $P = 0.945$) (**b**). **c,d**, Time spent interacting with male or female experimenter skin swabs versus control (water) swabs (CD1 mice; $n = 6$ experimenters per sex; $n = 24$ mice per sex; two-sided Wilcoxon matched-pairs signed-rank test; male swabs $P = 0.031$, female swabs $P = 0.031$) (**c**) and test versus habituation in the real-time place preference with experimenter and control t-shirts (CD1 mice; $n = 8$ experimenters per sex; $n = 16$ mice per sex; two-sided paired *t*-test; male t-shirts $P < 0.001$, female t-shirts $P = 0.049$) (**d**). **e**, Time spent in each arm of a Y-maze with male-, female- and water-scented swabs (CD1 mice; $n = 8$ experimenters per sex; $n = 30$ mice; two-sided repeated measures (RM) two-way ANOVA followed by Holm–Sidak correction, $P = 0.023$). **f**, Percentage change from habituation (CD1 mice; $n = 8$ experimenters per sex; $n = 30$ mice per sex, two-sided Kruskal–Wallis followed by correction with two-stage linear step-up procedure of Benjamini, Krieger and Yekutieli; control versus male $Q = 0.001$, male versus female $Q = 0.010$). **g**, Representative heat maps of mice shown in **h. h**, Conditioned place preference/aversion (CPP and CPA) of mice with male-scent-paired and female-scent-paired compartments (CD1 mice; $n = 8$ mice per sex; two-sided Mann–Whitney *U* test for CPA, $P = 0.038$; and two-sided unpaired *t*-test for CPP, $P = 0.831$). **i**, ROC curve includes all data in this figure ($P = 0.0031$). **j**, Latency to groom in the presence of male or female experimenter skin swabs (CD1 mice; $n = 13$ experimenters per sex; $n = 26$ mice per sex; two-sided Kolmogorov–Smirnov test, $P = 0.046$). **k**, Latency

to eat in the novelty-suppressed feeding test (CD1 mice; $n = 7$ experimenters per sex; $n = 28$ mice per sex; two-sided unpaired *t*-test, $P = 0.009$). **l**, Escape failures following inescapable shock training displayed by mice handled by male and female experimenters (CD1 mice; $n = 8$ experimenters per sex for male mice and $n = 8$ experimenters per sex for female mice; $n = 40$ female mice and $n = 40$ male mice per sex; two-sided RM two-way ANOVA, sex effect $P = 0.048$; and two-sided Mann–Whitney *U* test, $P = 0.012$). **m**, Contingency analysis of the number of stress-resilient and stress-prone mice (two-sided Fisher's exact test, $P = 0.0018$). Data shown are mean ± s.e.m. $^{*}P < 0.05$; $^{**}P < 0.01$; $^{***}P < 0.001$. For detailed statistical information, see Supplementary Table 1. VEH, vehicle.

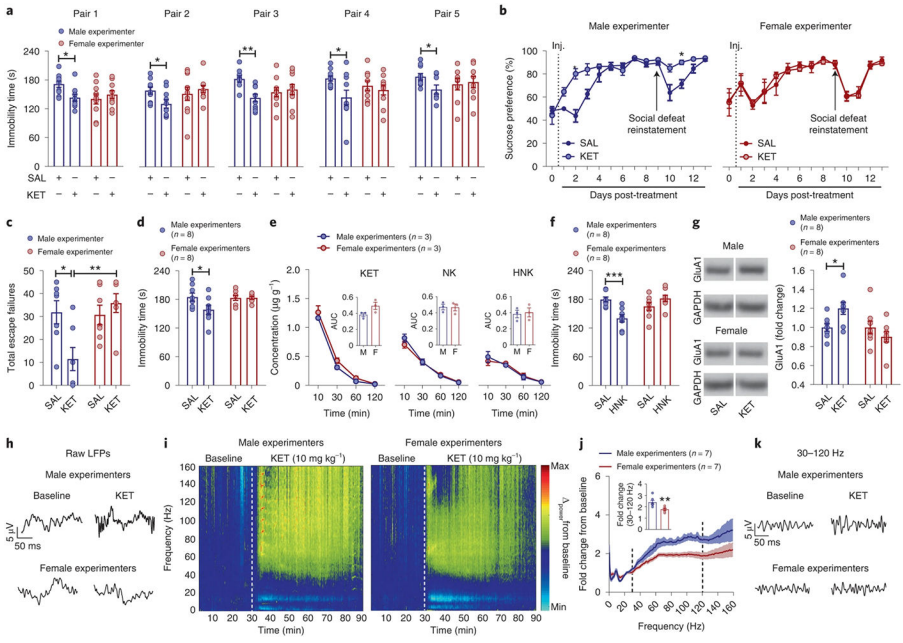

Fig. 2 |. The sex of the human experimenter influences antidepressant and electroencephalographic responses to KET.

a–c, Immobility time in the FST performed 1 h after dosing (CD1 mice; pairs 1, 2 and 4: n = 10 per treatment group; pair 3: n = 9, 10, 10, 10; pair 5: n = 10, 8, 9, 9; two-sided two-way ANOVA followed by Holm–Sidak test for pairs 1 and 3 and two-sided unpaired t-test for pairs 2, 4 and 5; pair 1: P = 0.024; pair 2: P = 0.024; pair 3: P = 0.008; pair 4: P = 0.025; pair 5: P = 0.030) (**a**), sucrose preference following social defeat (C57BL/6J mice; n = 7–6 mice per treatment group; two-sided Kruskal–Wallis followed by correction with two-stage linear step-up procedure of Benjamini, Krieger and Yekutieli; day 2: Q = 0.028; day 11: Q = 0.036) (**b**) and escape failures in the learned helplessness paradigm following administration of either KET or SAL by male versus female experimenter (CD1 mice; n = 7 per treatment group; two-sided two-way ANOVA followed by Holm–Sidak test; male SAL versus KET, P = 0.023; male KET versus female KET, P = 0.006) (**c**). **d**, Immobility time in the FST 1 h following either KET or SAL injections by male or female experimenters at another institution (CD1 mice; n = 8 experimenters per sex; n = 16 mice per treatment group; two-sided two-way ANOVA followed by Holm–Sidak test; P = 0.027). **e**, Brain concentrations of KET, norketamine (NK) and (*2R,6R;2S,6S*)-HNK following administration of KET (10 mg kg^{-1}; i.p.) by male or female experimenters (CD1 mice; n = 3 experimenters per sex; n = 12 mice per timepoint per sex). **f**, Immobility time in the FST 1 h following administration of (*2R,6R*)-HNK or SAL by male or female experimenters (CD1 mice; n = 8 experimenters per sex; n = 16 mice per treatment group; two-sided two-way ANOVA followed by Holm–Sidak test; P = 0.0008). **g**, Levels of GluA1 in ventral hippocampus. Blot images are cropped. The full gel images along with the molecular weight/size markers can be found in Supplementary Fig. 1 (CD1 mice; n = 8 experimenters per sex; n = 16 mice per treatment group; two-sided two-way ANOVA followed by Holm–Sidak test; P = 0.039). **h–k**, Representative qEEG local field potentials (LFPs) (**h**), spectrograms (**i**), fold change from baseline (CD1 mice; n = 7 experimenters per sex; n = 28–29 mice per treatment group; two-sided Mann–Whitney

U test; $P = 0.001$) (**j**) and representative traces from 30–120 Hz following administration of KET by male or female experimenters (**k**). Data shown are mean ± s.e.m. *$P < 0.05$; **$P < 0.01$; ***$P < 0.001$. For detailed statistical information, see Supplementary Table 1. Inj., injection.

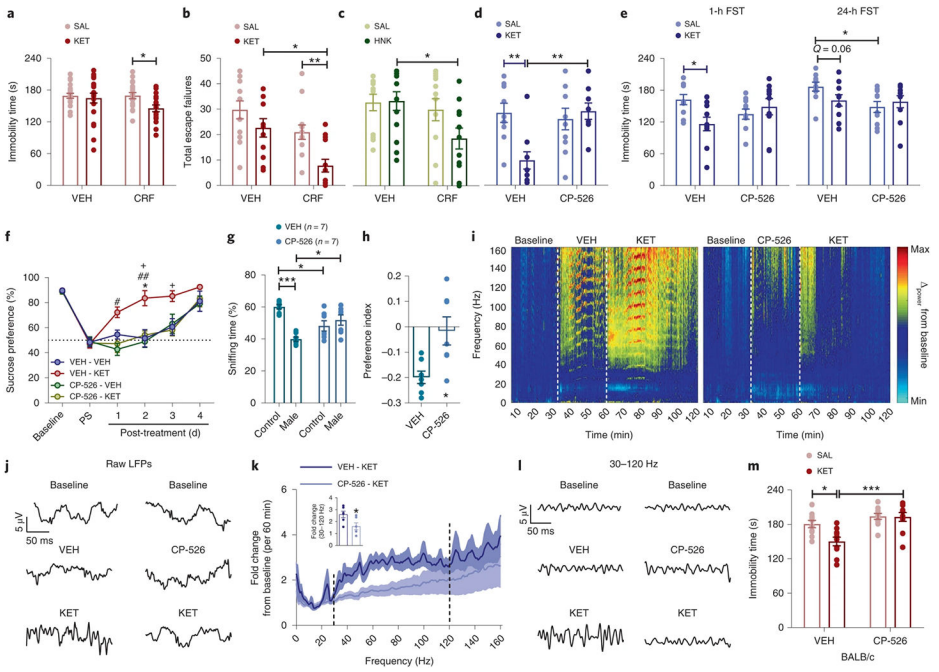

Fig. 3 | CRF mediates antidepressant responses to KET.

a–c, Effects of ICV administration of CRF before KET in the FST (CD1 mice; $n = 20, 18, 20, 18$ mice per treatment group; two-sided two-way ANOVA followed by Holm–Sidak test; $P = 0.036$) (**a**) and learned helplessness (LH) paradigm (CD1 mice; $n = 12–13$ mice per treatment group; two-sided Kruskal–Wallis followed by correction with two-stage linear step-up procedure of Benjamini, Krieger and Yekutieli; VEH-KET versus CRF-KET, $Q = 0.0086$; CRF-SAL versus CRF-KET, $Q = 0.0116$) (**b**) and before (*2R,6R*)-HNK administration in the LH paradigm by a female experimenter (CD1 mice; $n = 12, 12, 13, 11$ mice per treatment group; two-sided Kruskal–Wallis followed by correction with two-stage linear step-up procedure of Benjamini, Krieger and Yekutieli; $Q = 0.033$) (**c**). **d–h**, Escape failures (CD1 mice; $n = 9, 10, 10, 10$ mice per treatment group; two-sided two-way ANOVA followed by Holm–Sidak test; VEH-SAL versus VEH-KET, $P = 0.006$; VEH-KET versus CP-526-KET, $P = 0.004$) (**d**), immobility time (CD1 mice; $n = 10$ mice per treatment group; two-sided two-way ANOVA followed by Holm–Sidak test for 1 h, $P = 0.021$; and two-sided Kruskal–Wallis followed by correction with two-stage linear step-up procedure of Benjamini, Krieger and Yekutieli for 24 h, $Q = 0.026$) (**e**), CSDS-induced sucrose preference deficits (C57BL/6J mice; $n = 7$ mice per treatment group; two-sided Kruskal–Wallis followed by correction with two-stage linear step-up procedure of Benjamini, Krieger and Yekutieli for the treatment days; *VEH-KET versus VEH-VEH, $^{\#}$VEH-KET versus CP-526-VEH, $^{+}$VEH-KET versus CP-526-KET; day 1, VEH-KET versus CP-526-VEH, $Q = 0.0237$; day 2, VEH-KET versus VEH-VEH, $Q = 0.0165$; VEH-KET versus CP-526-KET, $Q = 0.0288$; VEH-KET versus CP-526-VEH, $Q = 0.0086$; day 3, VEH-KET versus VEH-VEH, $Q = 0.0506$; VEH-KET versus CP-526-KET, $Q = 0.0336$) (**f**) and skin swab preference (**g**) and preference index (**h**) following pretreatment with the CRF1 receptor antagonist CP-154,526 (CP-526) by a male experimenter (CD1 mice; $n = 7$ experimenters; $n = 28$ mice per treatment group; two-sided two-way ANOVA followed by

Holm–Sidak test for **g**; control VEH versus CP-526, $P = 0.0107$; control VEH versus male VEH, $P < 0.0001$; male VEH versus male CP-154.526, $P = 0.0107$; and two-sided unpaired *t*-test for **h**, $P = 0.0107$). **i–l**, Representative spectrograms (**i**) and traces (**j**) from raw LFPs, fold change (CD1 mice; $n = 6$ mice per treatment group; two-sided unpaired *t*-test, $P = 0.023$) (**k**) and representative 30–120-Hz traces derived from qEEG recordings from mice treated with CP-526 before KET (**l**). **m**, Effects of CP-526 administration before KET in BALB/cAnNCrl mice by a female experimenter ($n = 10$ mice per treatment group; two-sided two-way ANOVA followed by Holm–Sidak test; VEH-SAL versus VEH-KET, $P = 0.011$; VEH-KET versus CP-526-KET, $P = 0.0003$). Data shown are mean ± s.e.m. $^{*,\#,+}P < 0.05$; $^{**}P < 0.01$; $^{***}P < 0.001$. For detailed statistical information, see Supplementary Table 1. PS, post-stress.

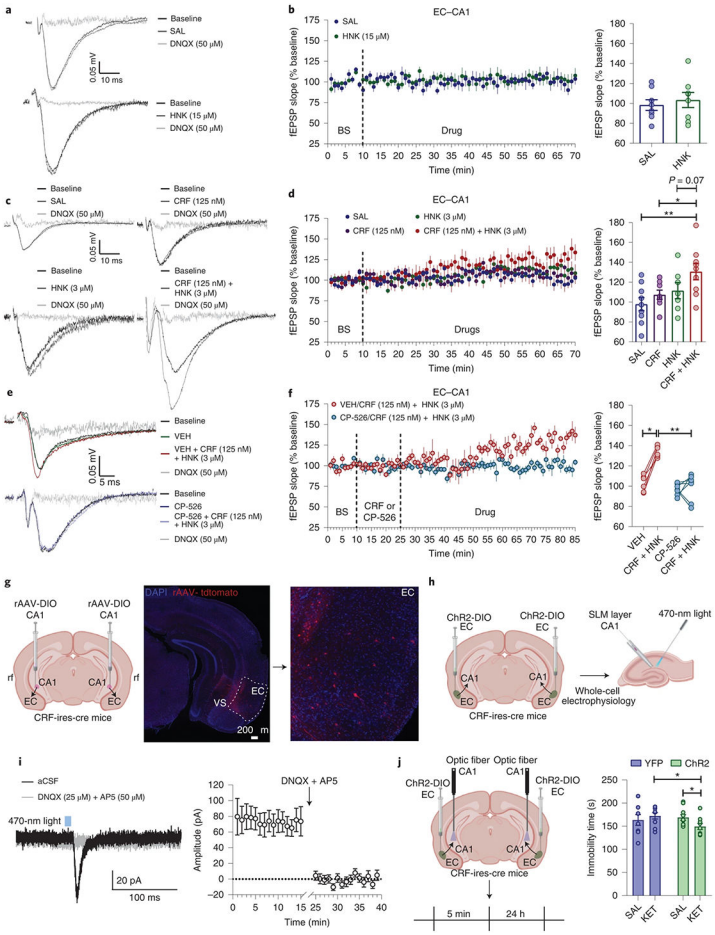

Fig. 4 | CRF mediates electrophysiological responses to (2R,6R)-HNK.

a–d, Representative traces (**a,c**) and quantification (**b,d**) of fEPSP slopes following stimulation of the EC–hippocampal CA1 (EC–CA1) pathway following wash-in of (**a,b**) SAL and (*2R,6R*)-HNK (C57BL/6J mice; $n = 8$ slices per group; two-sided unpaired *t*-test) or (**c,d**) SAL, CRF, (*2R,6R*)-HNK or CRF + (*2R,6R*)-HNK in a separate experiment (C57BL/6J mice; $n = 9, 8, 7, 9$ slices per group; two-sided one-way ANOVA; CRF + HNK versus SAL, $P = 0.0055$; CRF + HNK versus CRF, $P = 0.0495$). **e,f**, Representative traces (**e**) and quantification (**f**) of fEPSP slopes from the EC–CA1 pathway during pre-wash-in with the CRF1 antagonist CP-154,526 and wash-in with CRF + (*2R,6R*)-HNK (C57BL/6J mice; $n = 6, 6, 7, 7$ slices per group; two-sided Kruskal–Wallis followed by correction with two-stage linear step-up procedure of Benjamini, Krieger and Yekutieli; VEH versus CRF + HNK, $Q = 0.012$; VEH/CRF + HNK versus CP-526/CRF + HNK, $Q = 0.008$). **g**, Representative images from retrograde AAV-tdTomato injection in CRF-cre mice to the CA1 area and labeled projections in the EC (independently replicated in 3 animals). **h**, Experimental schematic. **i**, Representative traces of PSCs recorded from a CA1 stratum lacunosum moleculare (SLM) interneuron voltage clamped at −60 mV in response to optogenetic stimulation of the CRF-expressing EC–CA1 circuit before and after superfusion of the slices with DNQX + DL-AP5, and quantification of current amplitudes (CRF-cre mice; $n = 7$ cells from 4 animals). **j**, Experimental schematic and analysis of FST

performance following the optogenetic stimulation of the CRF-expressing EC–CA1 circuit before KET administration in a biosafety cabinet (CRF-cre mice; $n = 8, 10, 10, 9$ mice; two-sided Kruskal–Wallis followed by correction with two-stage linear step-up procedure of Benjamini, Krieger and Yekutieli for pre-selected comparisons; YPF KET versus ChR2 KET, $Q = 0.021$; ChR2 SAL versus ChR2 KET, $Q = 0.046$). Data shown are mean ± s.e.m. *$P < 0.05$; **$P < 0.01$. For detailed statistical information, see Supplementary Table 1. BS, baseline; rf, rhinal fissure; VS, ventral subiculum.

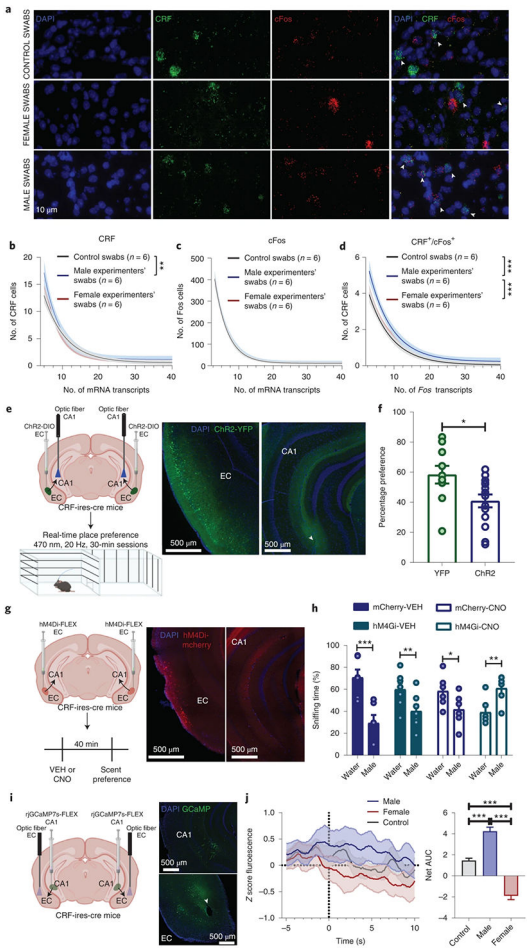

Fig. 5 | CRF-positive EC cells mediate aversion to male experimenters' scent.
a–d, Representative images (**a**) and quantification of *CRH*$^{+}$ (**b**), *Fos*$^{+}$ (**c**) and *CRH*$^{+}$/*Fos*$^{+}$ (**d**) cells in EC following exposure to experimenter scents (CD1 mice; $n = 6$ experimenters, $n = 12$ mice per group; two-sided extra-sum-of-squares; CRF: control versus male, $P = 0.008$; Fos/CRF: control versus male, $P < 0.0001$; male versus female, $P = 0.0001$). **e,f**, Schematic of the experiment and representative images (**e**), and quantification of the real-time place preference during optogenetic stimulation of the CRF EC–hippocampal CA1 (EC–CA1) pathway (CRF-Cre mice; $n = 10$, 14 mice; two-sided unpaired t-test, $P = 0.022$) (**f**). **g,h**, Experimental schematic and representative images (**g**), and quantification of the preference to the male experimenters' scent compared with control following chemogenetic inhibition of the CRF EC–CA1 pathway (CRF-cre mice; $n = 6, 7, 6, 6$ mice; two-sided mixed-effects three-way RM ANOVA followed by correction with two-stage linear step-up procedure of Benjamini, Krieger and Yekutieli; Water/mCherry-VEH versus Male/mCherry-VEH, $P < 0.0001$; Water/hM4Gi-VEH versus Male/hM4Gi-VEH, $P = 0.007$; Water/mCherry-CNO versus Male/mCherry-CNO, $P = 0.017$; Water/hM4Gi-CNO versus Male/hM4Gi-CNO, $P = 0.007$) (**h**). **i,j**, Experimental schematic and representative images (**i**) and quantification of the calcium transients of the soma of CRF EC–CA1 cells during a choice between male or female experimenter or water swabs using fiber photometry (CRF-cre; $n = 6$ mice; two-sided one-way ANOVA followed by Holm–Sidak test; control versus male, $P < 0.0001$; control

versus female, $P < 0.0001$; male versus female, $P < 0.0001$) (**j**). Data for **b,c** and **d** are one-phase exponential decay curves representing the mean ±95% confidence intervals. Data for **e–j** are shown as mean ± s.e.m. *$P < 0.05$; **$P < 0.01$; ***$P < 0.001$. For detailed statistical information, see Supplementary Table 1.